Computers and Electronics in Agriculture 222 (2024) 109037

Contents lists available at ScienceDirect

Computers and Electronics in Agriculture

journal homepage: www.elsevier.com/locate/compag

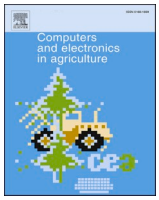

A systematic review of hyperspectral imaging in precision agriculture: Analysis of its current state and future prospects

Billy G. Ram [a], Peter Oduor [b], C. Igathinathane [a], Kirk Howatt [c], Xin Sun [a,*]

[a] Department of Agricultural and Biosystems Engineering, North Dakota State University, Fargo, ND 58102, USA
[b] Department of Earth, Environment, and Geospatial Sciences, North Dakota State University, Fargo, ND 58102, USA
[c] Department of Plant Sciences, North Dakota State University, Fargo, ND 58102, USA

ARTICLE INFO

Keywords:
Hyperspectral
Precision agriculture
Data analysis
Real-time
Image analysis

ABSTRACT

Hyperspectral sensor adaptability in precision agriculture to digital images is still at its nascent stage. Hyperspectral imaging (HSI) is data rich in solving agricultural problems like disease detection, weed detection, stress detection, crop monitoring, nutrient application, soil mineralogy, yield estimation, and sorting applications. With modern precision agriculture, the challenge now is to bring these applications to the field for real-time solutions, where machines are enabled to conduct analyses without expert supervision and communicate the results to users for better management of farmlands; a necessary step to gain complete autonomy in agricultural farmlands. Significant advancements in HSI technology for precision agriculture are required to fully realize its potential. As a wide-ranging collection of the status of HSI and analysis in precision agriculture is lacking, this review endeavors to provide a comprehensive overview of the recent advancements and trends of HSI in precision agriculture for real-time applications. In this study, a systematic review of 163 scientific articles published over the past twenty years (2003–2023) was conducted. Of these, 97 were selected for further analysis based on their relevance to the topic at hand. Topics include conventional data preprocessing techniques, hyperspectral data acquisition, data compression methods, and segmentation methods. The hardware implementation of field-programmable gate arrays (FPGAs) and graphics processing units (GPUs) for high-speed data processing and application of machine learning and deep learning technologies were explored. This review highlights the potential of HSI as a powerful tool for precision agriculture, particularly in real-time applications, discusses limitations, and provides insights into future research directions.

1. Introduction

Hyperspectral imaging (HSI) has emerged as a promising tool for precision agriculture (PA). Unlike common imaging techniques that use the visible spectrum (RGB) or multispectral data. HSI provides a more detailed and comprehensive view of crop health, allowing for more targeted and precise crop management decisions. By analyzing the unique spectral signature of crops, HSI can detect plant stress, disease, and nutrient deficiencies, providing valuable information that can be used to optimize crop yield and reduce input costs (Mishra et al., 2020). HSI utilizes the inherent property of materials to absorb a particular wavelength of light while reflecting or scattering other wavelengths. Interaction of objects with the electromagnetic spectrum is a universal phenomenon (Mishra et al., 2017b). HSI, therefore, provides a non-invasive method to detect molecular reflections and absorptions with the help of a wide range of wavelengths in the visible near-infrared (VNIR) and shortwave infrared (SWIR) regions of 400–2500 nm (Wieme et al., 2022). Understanding the patterns in molecular absorption and reflection and associating them with molecules present in the material (also known as study of spectroscopy) has been the focus of most research in the agricultural domain (Pavia et al., 2014).

HSI was predominantly used with orbital and suborbital platforms. Portable handheld variants of these sensors are now available and actively being used in fields of engineering, medical science research, and industrial production lines (Anastasiou et al., 2018; Picon et al., 2012; Tatzer et al., 2005). In the past twenty years, the number of peer-reviewed studies that use handheld variants of hyperspectral sensors are increasing, and more studies are building custom data collection platforms and analysis workflows (Fig. 1). This trend indicates a positive shift from geospatial applications to in-field applications, where data collection is conducted by users and automated analysis pipelines are

* Corresponding author.
E-mail address: xin.sun@ndsu.edu (X. Sun).

https://doi.org/10.1016/j.compag.2024.109037
Received 9 October 2023; Received in revised form 10 April 2024; Accepted 10 May 2024
Available online 17 May 2024

Nomenclature

1D CNN	1-dimensional convolutional neural network
3D CNN	3-dimensional convolutional neural network
AE-NN	autoencoder neural network
AI	artificial intelligence
AISA	airborne imaging spectrometer for applications
API	application programming interface
ARM	advanced RISC machine
AVIRIS	airborne visible/infrared imaging spectrometer
BIL	band interleaved-by-line
BIP	band-interleaved-by-pixel
BPNN	back propagation neural network
BSQ	band-sequential
CBD	canonical Bayesian discriminant
CCD	charge coupled diode
CDA	canonical discriminant analysis
CNN	convolutional neural network
CPU	central processing unit
CUDA	compute unified device architecture
DA	discriminant analysis
DCNN	deep convolutional neural network
DL	deep learning
DR	dimensionality reduction
DSP	digital signal processing
FCN	fully connected network
FLDA	fisher's linear discriminant analysis
FPGA	field programmable gate array
GBRT	gradient boosting regression tree algorithm
GPU	graphical processing unit
GTB	gradient tree boosting
HS-ANN	hybrid segmentation – artificial neural network
HSI	hyperspectral imaging
IR	infrared
KMNF	kernel minimum noise fraction
KNN	k-nearest neighbors
KPCA	kernel principal component analysis
LED	light emitting diode
LM	multi-variable linear regression
LPDBL	locally preserving discriminative broad learning
MCARI	modified chlorophyll absorption in reflectance index
ML	machine learning
ML/BSBC	maximum likelihood best spectral band combination
MLC	maximum likelihood classifier
MOG	mixtures of gaussians
MOG	mixture of gaussians
MSVM	multiclass support vector machines
NDVI	normalized difference vegetative index
NIR	near infrared
NN	neural networks
PA	precision agriculture
PCA	principal component analysis
PLB	potato late blight
PLS-DA	partial least square discriminant analysis
PLSR	partial least square regression
PRISMA	preferred reporting items for systematic reviews and meta-analyses
RBF	gaussian radial basis function kernel
RF	random forest
RFE	recursive feature elimination
RGB	red, green, and blue bands
ROI	region of interest
SAM	spectral angle mapper
SDA	stepwise discriminant analysis
SLOG	simple logistic
SMO	sequential minimal optimization
SOM	self-organizing maps
SPCA	standardized principal component analysis
SVM	support vector machine
SWIR	short wave infrared
TPE	tree-structured parzen estimator
UAV	unmanned aerial vehicle
UGV	unmanned ground vehicle
VCA	vertex component analysis
VNIR	visible near infrared

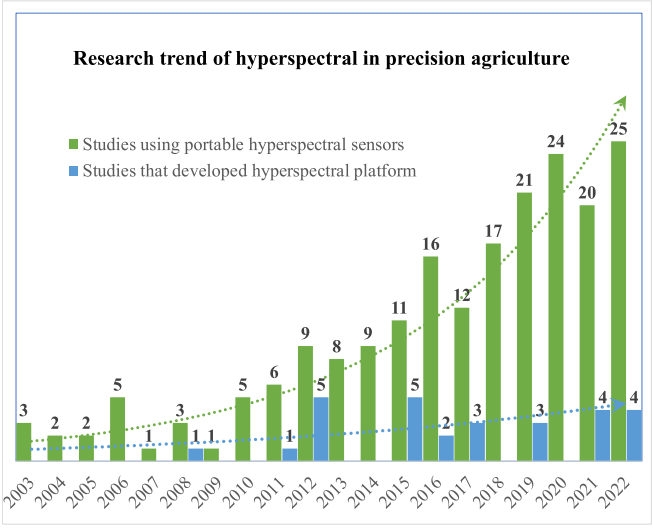

Fig. 1. Research trend in peer-reviewed publications showing the increasing trend of research with handheld hyperspectral sensors and custom platforms for hyperspectral data capture or analysis.

created for more real-time or near real-time applications.

Hyperspectral sensors, though constantly improving in the last many decades, still lack the ubiquitous feasibility to be applied in real-time applications as compared to the application of RGB cameras. Real-time application is defined as the collection of data and analysis as the data comes in, without the need for constant supervision of subject specialists (Merfield, 2016). It is a more machine-directed way of collecting and analyzing data. The impracticality of utilizing hyperspectral data stems from its high-dimensional data size, high cost and labor associated with data acquisition in comparison to digital images, and limited adaptation in the research community. For this reason, analysis of hyperspectral data is mostly done in research laboratories after exhaustive data processing and under the supervision of subject specialists. To overcome challenges in real-time applications of hyperspectral sensors, lessons learned in initial testing for various field applications, and further research are necessary. The focus also needs to be shifted towards technical methods that can bridge the gap created by handling high-dimensional hyperspectral data. Recent studies conducted in the review of HSI applications in agriculture have taken a broader perspective by including satellite, airborne sensors, UAV, and ground-based hyperspectral sensors (Lu et al., 2020), and focus more towards the working principles of HSI and their application in specific subject areas without inquiring about the technological advancements necessary. Table 1 shows the focus area of recent review studies conducted on

Table 1
An overview of significant hyperspectral imaging reviews conducted in the agricultural engineering domain in recent years.

Reference	Key aspects
Sanaeifar et al. (2023)	• Study of large-scale remote sensing models and proximal hyperspectral models. Applications of proximal hyperspectral in determining abiotic plant stress at leaf and canopy scale.
Barbedo (2023)	• Overview of working with hyperspectral data in each step of deep learning (DL) model development. DL applications in proximal HSI of vegetable production.
Eh Teet and Hashim (2023)	• Advantages and disadvantages of HSI for disease detection in fruits and vegetables. • Compares computer vision, multispectral, hyperspectral, biospeckle and thermal imaging. • Concludes suggesting the need for more standardization in data analysis procedures.
Ma et al. (2023)	• Efficiency of various spectroscopic sensors including HSI in the quality assessment of legumes. • Discusses computer vision and spectroscopic techniques.
Wieme et al. (2022)	• Quality assessment of fruit, vegetables, and mushrooms using HSI. • Machine learning (ML) and DL applications for assessment.
Khan et al. (2022)	• Implementation of Hyperion, Landsat-8, and Sentinel 2 satellite hyperspectral data in agriculture. • ML and DL methodologies are used in agriculture.
Berger et al. (2022)	• Reviewed early, medium, and chronic stages of plant stresses. • It concludes that NIR is one of the major tools used for plant stress detection.
Passos and Mishra (2022)	• Overview of DL parameters for spectral data. • Tutorial for hyperparameters tuning of DL models.
Wang et al. (2021)	• DL applications in HSI of plants. • DL models used with HSI. • Hyperspectral image analysis using DL models.
Lu et al. (2020)	• Application of satellite, aircraft, UAV, and proximal hyperspectral sensors in agriculture. • Data processing and analysis of data collected from various sensor types.
Mishra et al. (2020)	• Hyperspectral data collection of whole plants. • Illumination variations and correction approaches.
Benelli et al. (2020)	• Review of applications of ground-based HSI in precision agriculture for phenotyping, fruit ripening, chlorophyll, and Nitrogen content, drought stress, disease, and fungal detection.
Maes and Steppe (2019)	• Applications of hyperspectral sensors with UAVs. • Fusion of hyperspectral and thermal data for pathogen detection. • Comparison of RGB, multispectral, hyperspectral, and thermal for precision agriculture application.
Ali et al. (2019)	• Review of plant disease detection using different sensors. • Accuracy of proximal and remotely sensed HSI in disease detection.
Corti et al. (2018)	• Review of maize parameters influenced by N management using remote and proximal sensing. • The focus was on regression and vegetative indices analysis.
Tao et al. (2018)	• Use of fluorescence and near-infrared spectroscopy in real-time detection of fungal contamination in agricultural products. • Concluded that while near-infrared spectroscopy and HSI provide reliable results. High-dimensional data is a bottleneck problem for real-time sorting applications.
Mishra et al., (2017b)	• Application of proximal HSI in plants. • Overview of light interaction, instrument setup and spectral data analysis.
He and Sun (2015)	• Real-time detection of microbial contamination in agricultural and food products using HSI. • Suggests multispectral over hyperspectral after real-time applications. • The need for standardization of hyperspectral data analysis is suggested as a future trend.

the application of HSI in agriculture. These studies shared overarching goals with this review; however, our study is unique in the sense it focuses on the requirements for real-time applications of ground-based hyperspectral sensors and introduces necessary tools. Therefore, this study aims to concentrate only on ground-based, UAV, and aircraft-mounted hyperspectral sensors that have high spatial resolution. The reason to focus on just these sensors is that they provide more freedom for in-field integration with UAVs, UGVs, and platform ecosystems comprising multiple sensors while allowing high temporal resolution data recording. With the above goals, the objectives of this review study are:

Review literature from the past 20 years (2003–2023) that used portable hyperspectral sensors (ground-based, UAV, portable hand-held, and spectroradiometers) for applications in agricultural farmlands.
Clearly define the necessary resources that are needed for the real-time application of hyperspectral sensors.
Review the trends, explore the applicability, observe the real-time application of HSI, and suggest future research directions for successful implementation of HSI for real-time application in PA.

2. Methodology of literature selection for the review

A systematic review of published literature was conducted to address the real-time applications of hyperspectral sensors. Systematic review guidelines published under the Preferred Reporting Items for Systematic reviews and Meta-Analyses (PRISMA) were followed for the selection of literature (Page et al., 2021).

2.1. Eligibility criteria

For the review, literatures published in 2003–2023 was selected. Studies that use portable and/or high spatial resolution hyperspectral sensors were included. To facilitate a natural understanding of the topic, three main categories in hyperspectral data analysis that need to be addressed for real-time applications were identified. These were data collection, data processing, and applications. A flowchart of these categories with their sub-categories is shown in Fig. 2.

2.2. Search strategy and information sources

Four databases were used to search for literature. These were Web of Science, Scopus, Science Direct, and Google Scholar. Boolean operators ('AND' and 'OR') were utilized with search terms to narrow down the search results (Table 2). The search term "hyperspectral" gave multiple results that included work based on satellite hyperspectral, which was out of the scope of the study. To focus on proximal hyperspectral sensor literature, sensor manufacturer names generally found in literature along with special keywords were used. A complete list and search terms properly categorized can be found in Table 2. These search terms were used interdependently across categories.

2.3. Selection processes

Primary focus was on studies that use proximal hyperspectral sensors for agricultural applications. Studies that use ML or DL technologies along with technical novelty that improves either data analysis pipelines, or achieves real-time application of hyperspectral sensors, and studies that fabricate platforms that facilitate data collection or analysis were included. Automation tools found in the database search engine were used to narrow down the search results. Only literature published in the English language was included. Conference papers and literature published in different study domains were preferentially removed. Finally, 97 research articles were used for this systematic review. The complete literature screening process is displayed in Fig. 3.

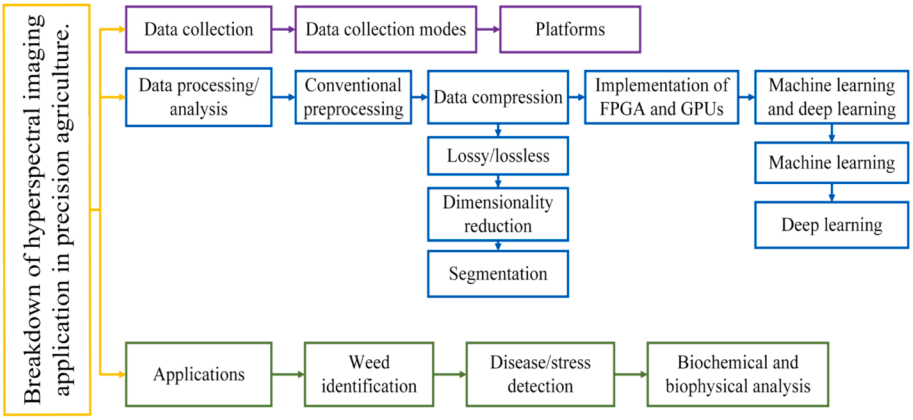

Fig. 2. Flowchart illustrating the outline of the systematic literature review study.

Table 2
Overview of different search criteria used to search for literature in Web of Science, Scopus, Science Direct, and Google Scholar.

Category	Search terms*
Study area	"agriculture" OR "precision agriculture" OR "smart agriculture"
Data collection	"specim" OR "headwall" OR "cubert" OR "resonon" OR "inno-spec" OR "hyspex" OR "ground hyperspectral" OR "infield hyperspectral" OR "proximal hyperspectral" OR "close range hyperspectral"
Data processing	"dimensionality reduction" OR "feature selection" OR "segmentation" "real-time" OR "in field" OR "automatic" OR "autonomous" "gpu" OR "graphical processing unit" OR "nvidia" OR "fpga"
Applications	"weed identification" OR "weed classification" OR "crop monitoring" OR "disease detection" OR "pest detection" OR "nutrient management" OR "biomass" OR "leaf area" OR "chlorophyll" OR "nitrogen" OR "stress"

*These search terms were used interdependently. For example, data collection terms with data processing terms, or data collection terms with applications terms.

3. Hyperspectral data collection

Data acquisition is an essential aspect of HSI, as there are several modes of data acquisition. These modes not only affect the various data resolutions but also determine their applicability in real-time scenarios.

3.1. Data collection modes

Data collection modes include line scan, point scan, wavelength scan, and snapshot scanning acquisition modes (Fig. 4). Each of these modes has its own advantages and disadvantages for real-time applications, data collection, analysis, and management (Adão et al., 2017).

Point scanning sensors (Fig. 4a) collect data at discrete points, providing very high spectral resolution albeit with no spatial information, since direct contact or proximity to the subject is required (Omidi et al., 2022; Qin, 2010). Line scan sensors (Fig. 4b), acquire data in a push-broom pattern and require a translation stage to capture the complete image. These sensors are commonly used for large-scale mapping, offering high data coverage, and low data redundancies (Fowler, 2014). As a result, the data size from point scan sensors is smaller compared to that of line scan sensors. Wavelength scan sensors (Fig. 4c) require a variable filter or spectrometer that distributes certain wavelengths. These filters are generally mounted on charge-coupled diode (CCD) sensors which are light-sensitive integrated circuits and significantly reduce the cost of hyperspectral data acquisition (Eddy et al., 2008). But their spectral dimension is limited to the specifications of the filters. Snapshot sensors (Fig. 4d) acquire data simultaneously

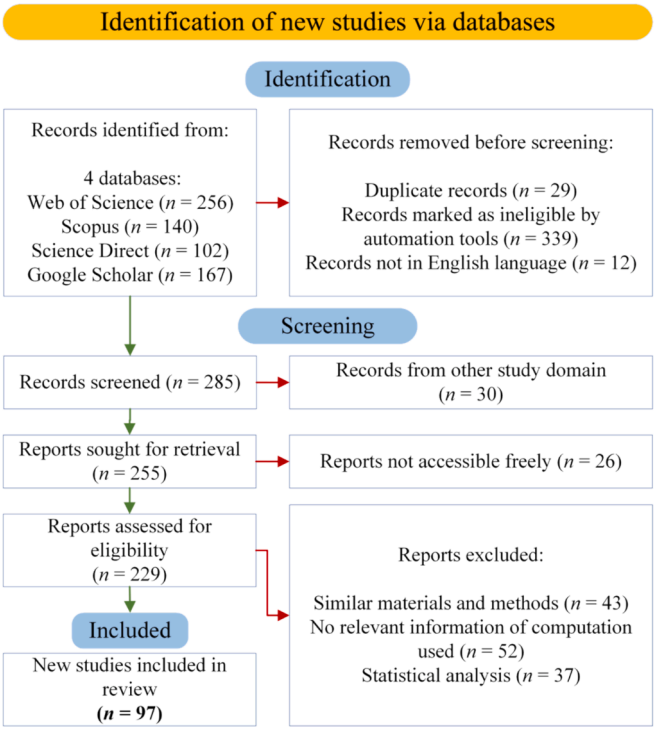

Fig. 3. Literature screening process according to PRISMA guidelines (Haddaway et al., 2022).

over the entire scene, offer high spatial, and spectral resolution, but require large amounts of data storage (Wong, 2009). Efficient data management is a crucial aspect of hyperspectral data acquisition, as the collected data can be quite large (Mishra et al., 2017b). The choice of data acquisition mode can impact the amount of data generated and the type of analysis that can be performed (Nie et al., 2023).

Line scan sensors are known to record distorted images once vibrations are introduced in the sensor or the object while data capture is in process, especially when using line scan sensors mounted on UAVs (Horstrand et al., 2019a). A comparative study of line scan and snapshot sensors mounted on UAVs done by Sousa et al. (2022) suggests that line scan sensors performed better as compared to the snapshot in terms of processing time, complexity, flight planning, and the ability to capture a whole spectral resolution at once. Line scan limitations include spatial distortions and a difficult orthorectification process. Recording more than a hundred wavelengths of spectral data can reduce the speed of data collection. Snapshot, line scan, and wavelength scan sensors can be

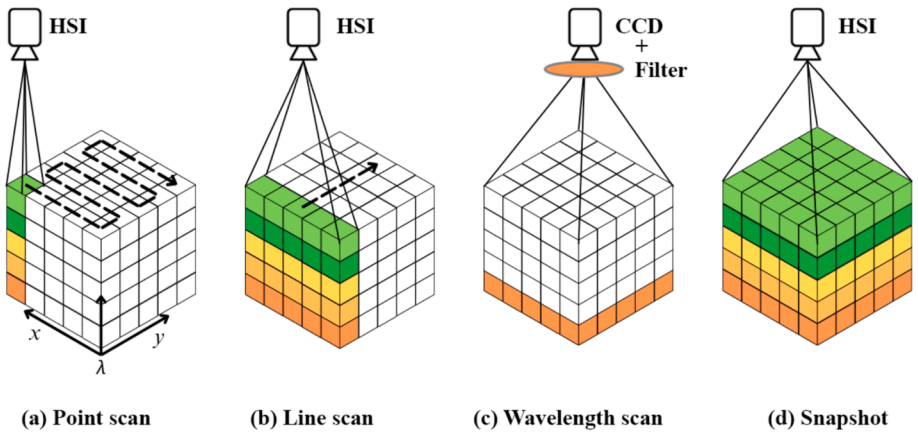

Fig. 4. Different modes of hyperspectral data collection. (a) Point scan, (b) line scan, (c) wavelength scan, and (d) snapshot scan.

used to utilize the spatial information along with the spectral information. Whereas point scan sensors mostly find their use in studies that utilize spectral information for biochemical analysis (see Fig. 5).

3.2. Hyperspectral platforms

Platforms that can support hyperspectral sensors for data collection and application in agricultural farmlands can help in the implementation of these sensors for various agriculture tasks. Essential parts of these platforms include a translation stage (in case of a line scan sensor), artificial light source to reduce variability, data recording computer, software to manage the data capture, data management, and platform mobility in the field (Mishra et al., 2020). Data collection platforms using line scan sensors face the problem of image distortion generated due to wind, while actively scanning. To limit these distortion effects, it is beneficial to collect data at no wind conditions or obstruct the flow of wind by completely covering the scanning area. Open structure platforms using line scan sensors are therefore limited by weather conditions (Eddy et al., 2008).

There are limited studies with hyperspectral platforms that can record data and analyze it simultaneously. Most of these studies are done in controlled environments and in closed system platforms. These systems help control the environment variability and commonly utilize a forward-feed technique. In which, the data is collected, stored in the computer, and models are deployed after training. As in the case of Mishra et al. (2022b), their all-in-one CPU based system facilitates data collection, has arrangements to set the field of view of the sensor and allows deployment of trained model for analysis with different data. Hyperspectral sensors that capture fewer bands instead of the usual hundreds of bands have been successfully used for real-time actuation tasks. Reduced data size combined with DL can achieve processing speeds of up to 0.04 s/image followed by sorting with a robotic arm (Chen et al., 2022). Working with limited bands has enabled micro dosing of weeds by using Bayesian classifiers with the help of platform mounted on tractor at a considerable ground speed of 0.04 m/s (Zhang et al., 2012b). Deploying hyperspectral sensors that can record 224 bands on a UAV has its own technical difficulties. Using embedded systems having multiple graphical processing units (GPUs) like the NVIDIA Jetson TX2 has facilitated hyperspectral data recording while wirelessly connected via a remote controller (Horstrand et al., 2019b). With these implementations, we are noticing a shift in hyperspectral applications in more complex environments.

The present state of hyperspectral studies utilizing platforms can be broadly classified as, (1) Data collection platforms: this is the basis of all platform designs and support mounting of sensor, and shutter triggers, with arrangements to block the external sunlight in case of ground-based systems. UAV-mounted sensors have been seen to utilize push-broom and snapshot sensors and collect data in solar radiance. The choice of hyperspectral mode of collection is highly dominated by push-broom sensors in ground platforms. No spectral data processing is conducted while data is recorded in both cases. (2) Actuation tasks platforms: these collect data and perform real-time tasks that include spraying, robotic arm manipulation, and real-time classification. While both push-broom and snapshot modes of data collection are used, hyperspectral data collected is highly reduced before actuation tasks with real-time speeds are performed. Real-time actuation platforms are currently limited to indoor-based systems only. Closed system hyperspectral data capture assures hassle-free data capture while also improving the ability for high temporal data collection.

3.2.1. Illumination requirements of platforms

HSI is a technique that records the interaction between light and an object across a broad range of the electromagnetic spectrum. The light-object interaction is dependent on the radiance energy of the incident light. It is observed that light absorbed in the visible range influences a molecule's electronic state. Interaction of light with molecules in the NIR and IR ranges introduces molecular vibrations which are beneficial to understand the physiochemical properties of plants (Edelman et al., 2012). Several illumination sources are available for HSI, including Halogen (Incandescent), Fluorescent, Light Emitting Diodes (LEDs), and Solar (Zahavi et al., 2019.). Hyperspectral Fluorescence Imaging utilizes fluorescent illumination that is in the range of 315–400 nm. Due to the small range of <100 nm, implementation of fluorescence imaging in agriculture is very limited (Kim et al., 2001). LED illumination is in the range of 380–700 nm. LED illumination provides a benefit of low working temperatures, low energy requirement compared to largely accepted Halogen illumination, and has been successfully used in seeds viability evaluation (Mo et al., 2014). It does not record interactions in the third overtone region that exist after 700 nm (Osborne, 1993). In the agricultural domain, halogen and solar illumination are used as preferred illumination sources (Table 3). Halogens have the advantage of being similar to solar illumination in terms of their continuous illumination range of 400–2500 nm. Hyperspectral platforms that use solar irradiance for data collection are often limited by the choice of vehicle, such as all UAVs use solar irradiance, and weather conditions, as windy conditions introduce distortions in image due to movement of plants while scanning using line scan sensors, and cloudy conditions. These platforms often record data at noon when solar radiance is at its highest (Eddy et al., 2008). Hyperspectral platforms that use halogen illumination reduce environmental variability and in almost all cases have an enclosure that helps negate the effects of wind on line-scan sensors.

3.2.2. Software for hyperspectral data acquisition and analysis

Hyperspectral data acquisition and analysis is predominantly

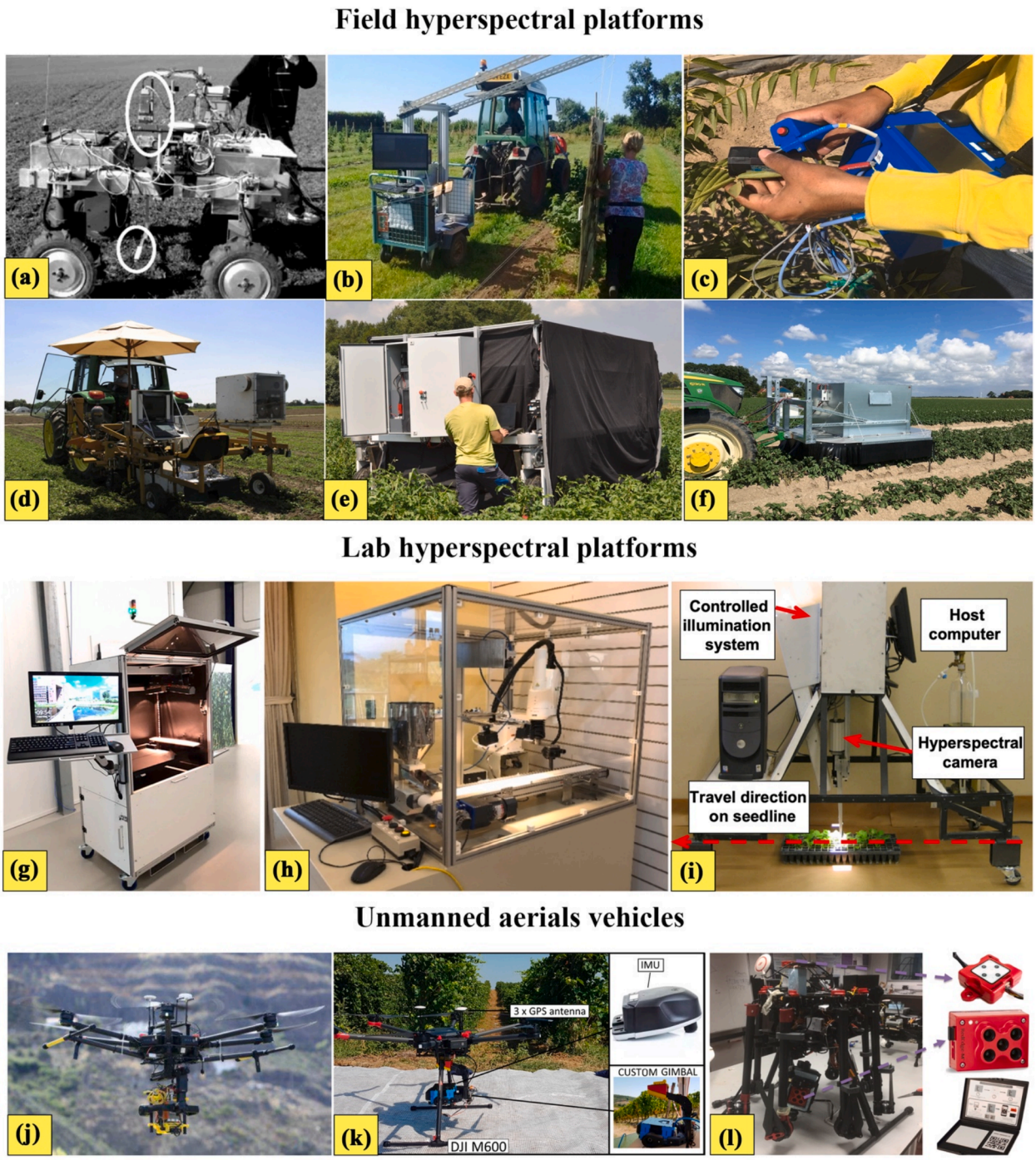

Fig. 5. Examples of hyperspectral platforms for field applications. (a) Autonomous Platform Information System (API) (Eddy et al., 2008); (b) Data collection with a person holding a cardboard background (Williams et al., 2017); (c) Two spectrometers fused to make a portable spectrometer running on Raspberry pi 3 for data collection (point scan method) (Omidi et al., 2022); (d and i) Platform for weed control with micro dosing capabilities, tested in field (d) and lab (i) conditions (Zhang et al., 2012a); (e and f) artificially illuminated systems for data collection Hypercart; (e) and imaging box; (f) (Polder et al., 2019; Van De Vijver et al., 2020), Examples of hyperspectral platforms for lab applications; (g) All-in-one spectral imaging (ASI) for data collection and model deployment (Mishra et al., 2022b); (h) Coffee bean defect inspection system with a robotic arm for sorting (Chen et al., 2022), Examples of hyperspectral platforms for aerial applications; (j) Data acquisition and recording powered with NVIDIA Jetson TK1 mounted on DJI Matrix M600 using Specim FX10 designed for ground applications (Horstrand and Guerra, 2019a); (k) DJI M600 mounted with UAV specific sensor with inbuilt data recording capability (Sousa et al., 2022); and (l) DJI S1000 with a Rededge multispectral sensor (Su et al., 2022).

performed using software supplied by the sensor manufacturer. Research utilizing proprietary software is constrained to offline operation, with data analysis being conducted separately, after the completion of data collection. The collected data is then processed through specific analysis pipelines, which may contain discontinuities and lack streamlining. The primary objective of real-time analysis is to eliminate these discontinuities. Support for data acquisition without commercial software is highly desirable but still lacking. Important tools for the development of these systems would be the availability of Application Programming Protocols (APIs), Software Development Kits (SDKs), and

Table 3
List of various hyperspectral platforms employed in agricultural applications.

Sensor	Vehicle	Application	Speed	Data recording	Range	Bands	Spatial resolution	Sensor type	Reference
Sony, ICX414AL with Linear Variable Filter	Tractor boom mounted[s]	FDC	–	Computer	400–1000 nm	61	640 × 480 px	Line Scan	Eddy et al. (2008)
ImSpector V8	Lab-Field system[h]	Micro dosing of weeds in real-time	0.04 m/s	Computer	384–810 nm	71	Rms spot radius < 30 μm	Line Scan	Zhang et al., (2012a); Zhang et al., (2012b)
Hamamatsu S9227-03 CMOS	Motorised Quadbike	Plant-Ground Discrimination	0.83 m/s	Computer	648–785 nm	3	6.4 mm	Line Scan	Symonds et al. (2015)
ImSpector N25E	Closed Lab System[h]	LDC	–	Computer	1000–2500 nm	288	rms spot radius < 15 μm	Line Scan	Wei et al. (2015)
HySpex VNIR 1600–160	Tractor mounted[s]	FDC	–	Computer	400–1000 nm	160	0.5 mm	Line Scan	Vigneau et al. (2011)
Inspector V9	UGV[s]	FDC	0.09 m/s	Computer	435–834 nm	200	4.8 × 6.4 mm	Line Scan	Pantazi et al. (2016)
Hyperspec Inspector VNIR	Fixed Site Gantry[h]	HTTP	46–80 plots/hr	Computer	400–1700 nm	923	1600 px	Line Scan	Virlet et al. (2017)
Hyperspec Inspector ExVNIR						229	320 px		
VNIR Gilden Photonics	Tractor Mounted[s]	FDC	2.7 m/s	Computer	400–896 nm	178	402 px	Line Scan	Williams et al. (2017)
SWIR Specim					895–2506 nm	278	378 px	Line Scan	
Specim FX10	DJI M600[s]	FDC	18 m/s	On board	400–1000 nm	224	1024 px	Line Scan	Horstrand et al., 2019b
Specim FX10	Tractor Mounted[h]	FDC	0.08 m/s	Computer	400–1000 nm	224	1024 px	Line Scan	Polder et al. (2019)
Imspector V9	Mobile Frame[h]	FDC	–	Computer	430–900 nm	200	0.30 mm/ pixel	Line Scan	Van De Vijver et al. (2020)
ImSpector V10E-PS	Electric Forklift[s] (Gantry like setup)	FDC	–	Computer	360–1025 nm	520	Rms spot radius < 9 μm	Line Scan	Jiang et al. (2021)
Imec XIMEA	Closed Lab System with Robotic Arm[h]	Defect inspection and sorting	0.04 s/ image	Computer	660–980 nm	25	216 × 409 px	Snapshot	Chen et al. (2022)
Specim FX10	Closed Lab System[h]	Data collection and model deployment	0.03 m/s	Computer	400–1000 nm	224	1024 px	Line Scan	Mishra et al., (2022b)
Flame-S + Flame-NIR	Handheld[h]	FDC	–	On Sensor	186–1700 nm	–	–	Point Scan	Omidi et al. (2022)
Senop HSC-2	DJI M600[s]	FDC	–	On Sensor	500–900 nm	1000	1024 px	Snapshot	Sousa et al. (2022)
Nano-Hyperspec					400–1000 nm	272	640 px	Line Scan	
RedEdge multispectral	DJI S1000[s]	FDC	1 m/s	On Sensor	475–840 nm	5	1.16 cm/px	Spectral Scan	Su et al. (2022)

FDC: Field Data Collection, LDC: Lab Data Collection, [s]: Solar Illumination, [h]: Artificial Illumination: Halogen. The Nomenclature should be referred for the additional abbreviations.

sensor compatibility with interfaces like GigE, USB 3.0, and PCIe. Pleora eBUS SDK has enabled GigE version sensors to communicate with ARM-based systems that have enabled the mounting of hyperspectral sensor on UAVs with data transfer compatibility (Horstrand et al., 2019a). Open-source language, e.g., Python has community developed libraries like Plant CV and Spectral Python (SPy) for hyperspectral data analysis (Fahlgren et al., 2015). Commercial software like MATLAB has support for toolboxes like HYPER-Tools available from its author's website, for analysis of hyperspectral data including segmentation, preprocessing, and classification (Mobaraki and Amigo, 2018). Another approach has been to use monochrome sensors with variable filters. The use of CCD sensors like Sony ICX414AL and Photometrics CoolSNAP$_{cf}$ sensor coupled with a linear variable filter or spectrograph (ImSpector V8) has enabled line scan data collection in various spectral ranges. The use of CCD sensors not made specifically for hyperspectral data collection has resulted in reducing the data collection cost and development of automated pipelines by allowing the collection of hyperspectral data with the same digital image pipelines (Eddy et al., 2008; Zhang et al., 2012a).

4. Data processing and analysis of hyperspectral data

While hyperspectral images are distinguished because of their multi-dimensional data, it is also accursed by it, as Bellman (1957) opined "this multidimensional data is burdened with the curse of dimensionality," which means that the data is laden with noise and has impractical data size. The noise in data can be generated due to the sensor's calibration, atmospheric effects, scattering of light, and plants geometric parameters. Therefore, pre-processing of hyperspectral data becomes crucial before any useful information can be extracted. The shift from satellite to proximal sensors has also seen a shift in the way data is preprocessed. Satellite hyperspectral data was predominantly pre-processed for atmospheric corrections and orthorectification. On the other hand, the raw spectral data from a proximal sensor is affected by scattering effects due to plants geometry (Mishra et al., 2020). Scattering introduces non-linearities in the data also known as multiplicative scale effects and commonly referred to as "scatter effects." Some of these preprocessing methods include normalization, multiplicative scatter correction, and Savitzky Golay filtering (Isaksson and Næs, 1988; Rinnan et al., 2009; Savitzky and Golay, 1964).

Preprocessing techniques can reduce the complexity of high-dimensional data, but they themselves do not meet the requirements of real-time applications. To achieve real-time processing, it is necessary to review and improve the use of data compression, on-board processing, and GPU processing in the analysis of hyperspectral data.

4.1. Conventional method of hyperspectral data analysis

Conventional analysis method follows a forward feed method of hyperspectral data analysis. Hyperspectral image cube (Fig. 6a) or point spectra (Fig. 6f) is acquired, followed by white and dark reference calibration, segmentation (Fig. 6d), spectral preprocessing (Fig. 6e, f), feature selection, unfolding of data i.e., converting a 3D image to a 2D table filled with reflectance values and using it as input for analysis. Many studies in the agricultural domain apply conventional preprocessing of hyperspectral data. The steps of acquiring and analysis of hyperspectral data are often broadly similar and change with respect to the choice of sensor and mode of data collection. Data is recorded using manufacturer-provided software. These methods of analysis completely focus only on the spectral data.

Point spectrometers do not capture the spatial information; therefore, no segmentation of data is required. These pure spectral signatures are used as input for analysis to determine equivalent object parameters. Which in the case of crops can be relative water content, and leaf mass per area (Junttila et al., 2022). Most studies do not use hyperspectral cubes from line scans or snapshot sensors directly even if the data is being recorded with a handheld device (Atsmon et al., 2022). They, at a minimum, apply background removal and image calibration before unfolding the images. Eventually, this leds to working with the spectral data only. Classification studies using spectral data focus on finding the best preprocessing method or methods to achieve the best model accuracy (Ahmed et al., 2022). Some studies also draw inferences by calculating various vegetative indices from the spectral data (Thorp et al., 2015). Overall, conventional analysis of hyperspectral studies uses a brute force approach for analysis of spectral data. Once spectral data is extracted from ROIs various ML and statistical models are used to draw inferences and classification results. Many studies use these classification results to suggest that real-time applications are possible, and they generally conclude that hyperspectral sensors can differentiate objects based on their chemical composition (Eddy et al., 2014). DL has shown potential to streamline hyperspectral analysis as discussed in detail in Section 4.4.

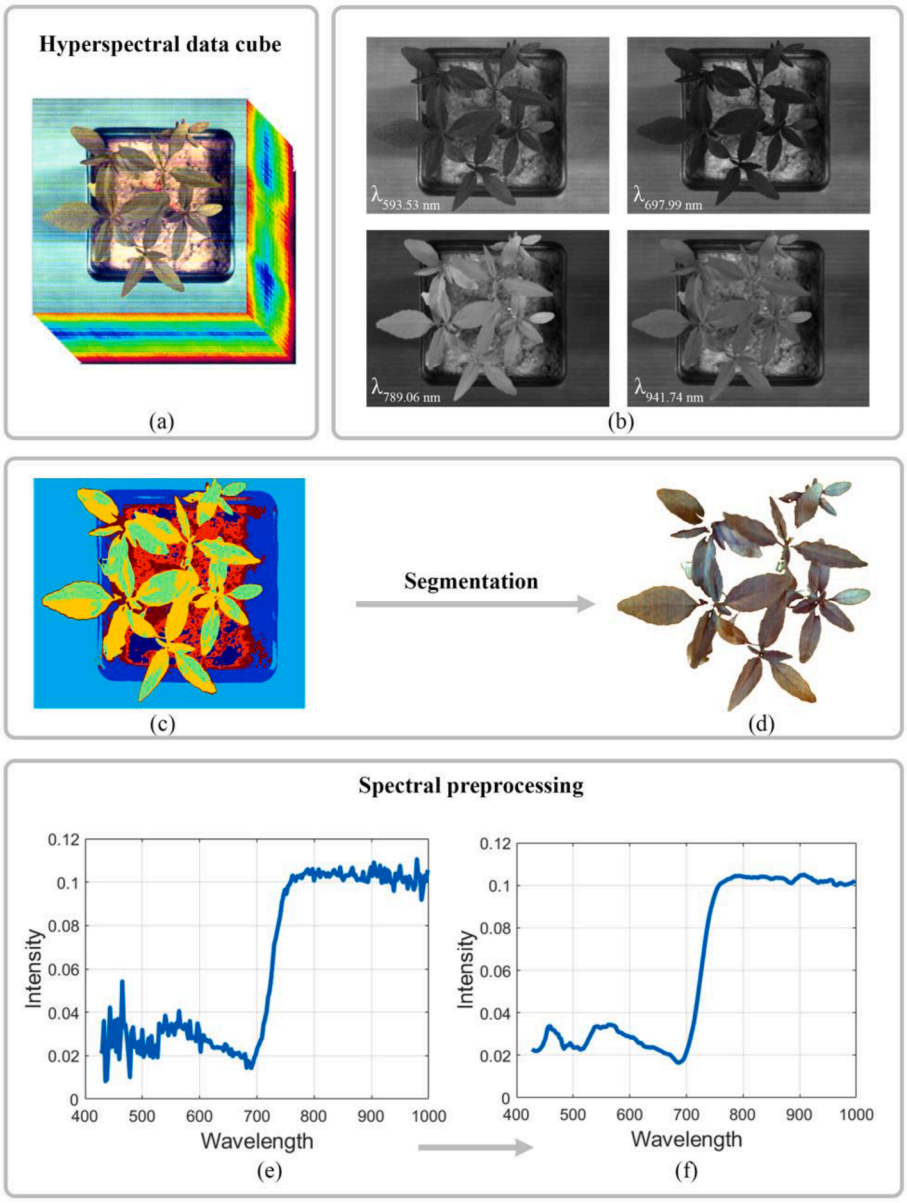

Fig. 6. (a) A visualization of a hyperspectral data cube. (b) Hyperspectral images from different wavelengths. The image at 789.06 nm can be clearly seen to show more reflectance in the crop foliage as compared to other wavelengths. (c-d) Showing a basic segmentation process using k-means clustering to remove the background. (e) Shows a raw crop spectral signature and, (f) shows the same spectral signature after preprocessing using Savitzky Golay 2nd derivative as an example.

4.2. Hyperspectral data compression

Hyperspectral data compression is necessary due to the multiple bands of spectral information. Multiple bands increase the data size, contribute to technical difficulty in data analysis, data storage, and real-time applications (Kaarna et al., 2007). For real-time applications of hyperspectral data, compression of multidimensional data is necessary and needed (Díaz et al., 2019).

4.2.1. Lossy and lossless data compression

Data compression techniques can be categorized in two ways as lossy, and lossless data compression (Miguel et al., 2006). In lossy data compression, redundant and irrelevant information from the data is permanently removed. Whereas in lossless data compression, no recorded data information is lost, and the data is accessible after decompression. Lossless data compression has the disadvantage of having less compression ratio than lossy data compression (Barrios Alfaro et al., 2020; Luo et al., 2022). Compression techniques can be further divided into transform-based, prediction-based, vector quantization, compressive sensing, tensor decomposition, sparse representation, multi-temporal, and learning-based (Dua et al., 2020). Compression based on hardware acceleration found that unmixing-based algorithms gave higher compression ratio while also being computationally demanding while prediction-based compression gave faster results (Altamimi and Ben Youssef, 2022)). Furthermore, most of these methods have been utilized with satellite or airborne hyperspectral sensors and must be thoroughly evaluated for their effectiveness with ground-based hyperspectral sensors. As the data from these platforms share a similar structure, it does not pose any challenges in the application of these methods to ground-based sensors. As suggested by the implementation of HyperLCA algorithm with AVIRIS (aircraft-based sensor) as well as Specim FX10 (ground-based sensor) hyperspectral data (Díaz et al., 2019). DL convolutional networks such as M2H-Net are used for the reconstruction of multispectral images to hyperspectral images and the concept of reconstruction has helped with data compression and data transfer; where a small amount of data can be stored and later reconstructed for use (Deng et al., 2021). The concept of hyperspectrogram for data compression is also currently being used (Corti et al., 2017). A hyperspectrogram is a visual representation of hyperspectral images that is created by combining the frequency distribution curves of score vectors from a principal component analysis (PCA) model. It is calculated separately on each hyperspectral image, can retain spatial information, and has been seen to achieve multifold reduction in data size using hyperspectrogram. For example, in a study by Corti et al. (2017), the raw image size of 1.25 GB, which when unfolded was sampled to 922 MB, and was further reduced to 300 kB by using hyperspectrogram. Examples of lossy data compression include spectral binning and dimensionality reduction (also known as feature selection). Binning helps decrease the cardinality of both continuous and discrete data. It has been successfully implemented in controlling data transfer speeds between the sensor and computer. Field implementation of spectral binning for data transfer has achieved real-time speeds of 0.036 m/s (Zhang et al., 2012a). While data compression is important, it is not a complete solution to the problem of high dimensionality as noticed by Okamoto et al. (2007), who used a wavelet transformation for compressing data collected from a point spectrometer (ImSpector V10). They suggested that dimensionality reduction is a crucial part of compressing data size.

4.2.2. Dimensionality reduction

Dimensionality reduction is a lossy method of hyperspectral data compression. It is one of the most common pre-processing steps applied to hyperspectral data. The main reason for this is not just the high-dimensional size but the redundant information recorded in the subsequent wavelengths. Redundancy does not add much information to the analysis but ends up overfitting the analysis model. Conventional workflows select significant bands and then use reduced data for their analysis. In most cases, dimensionality reduction brings the spectral dimension of the HSI image to less than fifteen bands (Gao et al., 2020). In some cases, less than five bands are also observed. An argument can be made that working with 10 or fewer bands of data for analysis is the same as working with multispectral sensors, and hyperspectral data is not required in such cases. While it is technically correct, multispectral sensors come with a fixed set of wavelengths. These pre-selected few wavelengths might not offer significant distribution among different objects, and therefore are limited to being used by objects of similar reflectance properties (that is, only with objects that have good reflection with those preselected fixed wavelength bands). But hyperspectral sensors provide the ability to investigate, narrow down significant wavelengths, and therefore can be applied to a wide range of objects. Therefore, dimensionality reduction with hyperspectral sensors is performed after investigation of the most significant wavelengths with respect to a particular material, and then reduced spectral data is applied for analysis. Whereas, in the case of multispectral sensors, there is no investigation step of significant wavelength involved.

There are two families of feature selection methods, namely, filter and wrapper (Su et al., 2022). Filter methods evaluate the relevance of each feature based on statistical measures and select the top features. Wrapper methods evaluate the performance of an ML algorithm to select the best combination of features (Li et al., 2011). Support vector machine (SVM) – multiclass forward feature selection with uninformative variable elimination achieved the fastest runtime of 17 s (Deng et al., 2013). Stepwise regression analysis and rank features technique have been used in studies on stomatal conductance (Jarolmasjed et al., 2018). In a comparison of five feature selection methods, it was noted that recursive feature elimination, which is a wrapper method, gave better prediction results than chi-square and *SelectFromModel* for disease identification in peanut plants (Wei et al., 2021). Current literature does not provide a standard feature selection algorithm or method. Instead, various methods are selected based on results obtained on homogenous data by researchers.

4.2.3. Image segmentation or background removal

Segmentation involves dividing an image into multiple segments or regions, each representing a homogeneous area with similar spectral properties (Fig. 6c). This step is often the first preprocessing step after image calibration in the analysis of hyperspectral images and plays an important role in improving the accuracy and efficiency of the subsequent analysis. This also ensures clean spectral data of objects for ML and DL models. Segmentation is used to remove the background (Fig. 6d), reduce the complexity, and enhance the performance of subsequent analysis and classification tasks (Eddy et al., 2008). To some extent, it also helps to reduce the data size, making it easier to process and analyze (Li et al., 2021). Ground hyperspectral image segmentation can be performed using various techniques, including clustering, morphological operations, and edge detection. PCA and vegetative indices like normalized difference vegetative index (NDVI) are used for the automated segmentation of plants with respect to ground (Williams et al., 2017), along with DL models trained on RGB images. This involves working with a pseudo-RGB image of the hyperspectral cube and generating a logical mask that can be applied to the hyperspectral cube. The choice of segmentation method depends on the specific requirements of the analysis and the type of data being processed (García-Santillán et al., 2017). Image segmentation is important in studies that work with reflectance values as it allows to keep the reflectance values of ROIs pure by removing reflectance values from surrounding areas.

4.3. Implementation of FPGA and GPUs with hyperspectral sensors

To ensure the efficient processing of large amounts of hyperspectral data, many researchers have explored the use of field programmable gate arrays (FPGAs) and GPUs (Fig. 7) in the implementation of ground

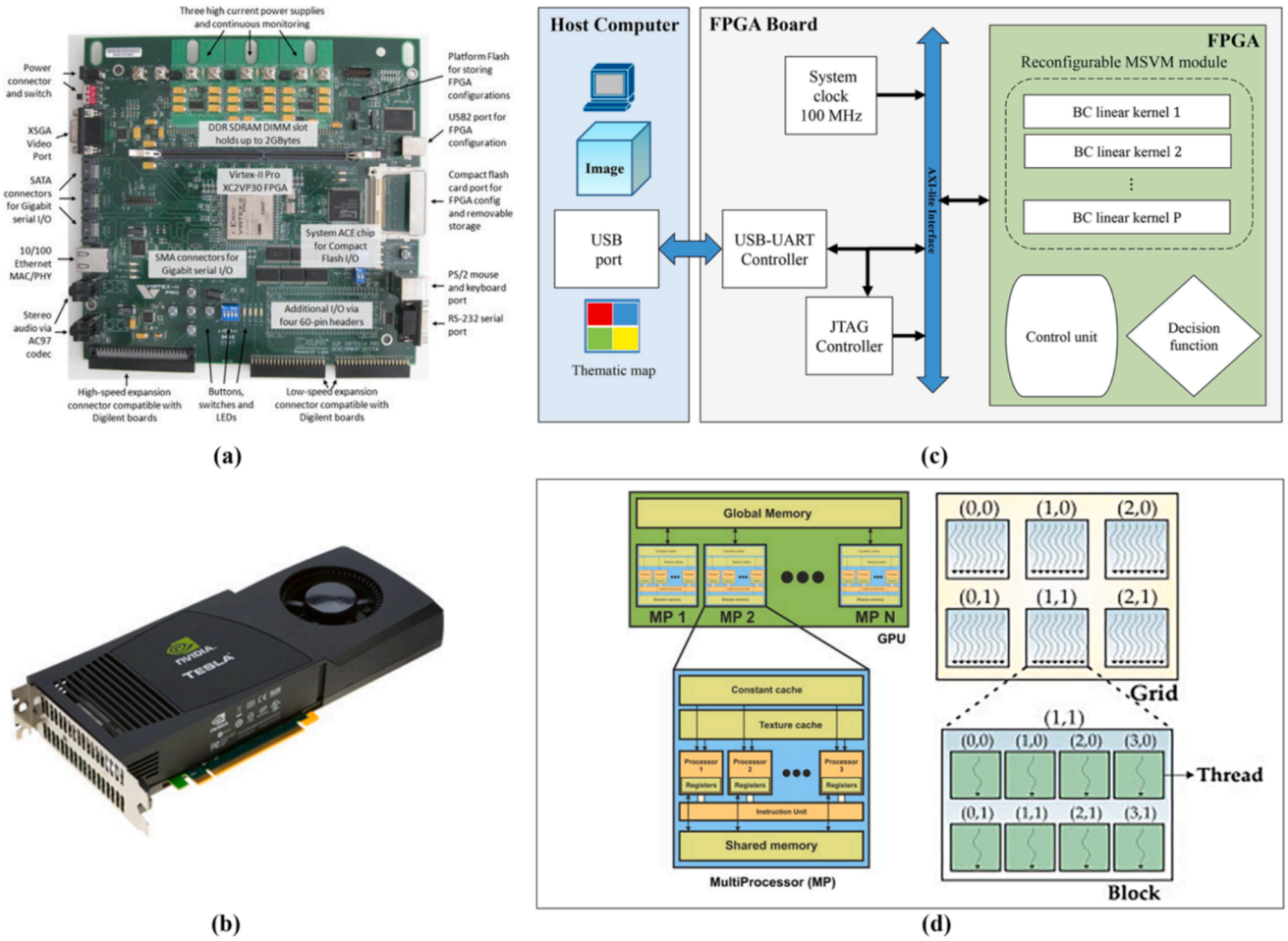

Fig. 7. Commercially available (a) FPGA, Xilinx reconfigurable board XUPV2P and, (b) NVIDIA Tesla C1060 GPU. (c) Architecture overview of an online-classification framework with FPGA. (d) GPU architecture showing batch processing capabilities on multiple threads. (González et al., 2013; Gyaneshwar and Nidamanuri, 2022).

hyperspectral sensors (Fenzandez et al., 2016). FPGAs are integrated circuits that can be reconfigured after manufacturing, allowing for custom logic design and redesign (Rosario et al., 2014). This flexibility makes FPGAs well-suited for the processing of hyperspectral data, as they can be configured to perform specific image processing tasks. For instance, FPGAs have been used to implement hyperspectral data compression algorithms (Nascimento and Vestias, 2016), reducing the amount of data that needs to be transmitted and stored. It has also been used to perform real-time data processing, enabling on-the-fly analysis of hyperspectral data during data collection. Recent advancements in the field have led to a significant increase in processing speed for hyperspectral images. Specifically, the use of a system-on-chip (SoC) FPGA has resulted in processing times that are 216 times faster for hyperspectral images of size ($512 \times 614 \times 224$) when compared to a 256 core GPU (Nascimento et al., 2020). GPUs are specialized processors designed to handle the complex calculations required for graphics processing (Díaz et al., 2019). It has been found to be highly effective for a wide range of hyperspectral data processing tasks (Gao et al., 2016), including image classification, and dimensionality reduction. GPU-accelerated algorithms have been shown to be much faster than traditional CPU-based algorithms, enabling the processing of large amounts of hyperspectral data in real-time (Horstrand et al., 2019a). Furthermore, the use of GPUs allows for the implementation of sophisticated algorithms, such as deep neural networks (Bouguettaya et al., 2022). The use of FPGA and GPU in the implementation of ground hyperspectral sensors has proven to be highly effective in improving the processing speed and accuracy of hyperspectral data (Table 4). These technologies have enabled new applications of hyperspectral sensors, including real-time data analysis and the implementation of complex algorithms (Horstrand et al., 2019a). As the demand for real-time analysis of hyperspectral data continues, the use of FPGA and GPU in hyperspectral data processing is expected to become even more widespread in the future. Implementation of multiclass support vector machines (MSVM) on low complexity FPGA (Artix-7) is said to achieve real-time classification speeds on datasets captured using airborne and ground hyperspectral sensors (Gyaneshwar and Nidamanuri, 2022). In some instances, FPGAs have also outperformed embedded GPUs from NVIDIA in their implementation of compression algorithms.

4.4. Machine learning and deep learning applied to hyperspectral data

ML and DL are two specializations in artificial intelligence that are increasingly being used in the analysis of data from ground hyperspectral sensors (Jordan and Mitchell, 2015). Both technologies have been utilized in the agricultural domain for various applications, including studying crop yield, diseases, and pest detection, performing classification tasks, and monitoring crop growth (Table 5). ML models rely on spectral data and do not incorporate spatial information. DL, a subset of ML, has enabled the integration of spatial information with spectral data. However, there are variations like one-dimensional convolutional neural networks (1D-CNN) within DL that also utilize only spectral information.

ML algorithms, such as decision trees (DT), random forests (RF), and SVM, can be used to classify hyperspectral data into different categories,

Table 4
Research articles that used FPGA and GPUs for their analysis.

Sensor name	Algorithm/ technique	Findings	Authors
AVIRIS	PCA on FPGA	Compared to a CPU, an FPGA achieved a speed increase of 10.08 s.	Fenzandez et al. (2016)
	PCA	Real-time functionality was achieved by applying the complete unmixing chain on a NVIDIA GPU Tesla C1060 architecture.	Sanchez and Plaza (2011)
	N-FINDR algorithm	The test machine demonstrated high scalability for band selection using GPU-based parallel implementations.	Yang et al. (2011)
	VCA on FPGA	The endmember extraction was achieved without the need for a dimensionality reduction preprocessing step.	Rosario et al. (2014)
	HySime	When comparing the HySime algorithm with CPU, GPU, and DSP, it was found that the GPU performed better.	Torti et al. (2014)
	G-OMNF	The proposed GPU implementation demonstrated the ability to perform in real-time with hyperspectral data sets.	Sanchez and Plaza (2011)
	VCA	Achieved unmixing without dimensionality reduction.	Nascimento et al. (2015)
	PCA on FPGA	Achieved 90 % more speed implementing PCA on FPGA vs CPU.	Fenzandez et al. (2016)
	VCA on FPGA	Proposed an FPGA-based architecture for extracting endmember signatures using a fully automatic VCA method that does not require a dimensionality reduction preprocessing step.	Nascimento and Vestias (2016)
	SpeCA	Parallel implementation of SpeCA on GPUs using the Compute Unified Device Architecture (CUDA), achieving 21x times more speed.	Sevilla et al. (2016)
	KPCA	KPCA (Kernel PCA), a nonlinear dimensionality reduction method, and proposed a parallel KPCA algorithm (KPCA-G) based on the CPU/GPU heterogeneous system.	Zhou et al. (2017)
	FastICA	Results show that their parallel implementations have excellent performance and scalability, achieving real-time HSI dimensionality reduction on a heterogeneous platform.	Fang et al. (2017)
	SPCA	Object-linked intelligent classification method for onboard classification of hyperspectral images, utilizing simpler neural networks and processes were proposed.	Mishra et al., (2017a)
	Multilayer perceptron	Compared algorithms execution and speedup time for CPU and GPU and found GPU to perform exponentially faster with 75 band images.	Penalver et al. (2017)
	PCA	The author discusses the implementation of PCA on a NVIDIA GPU and a Kalray manycore, highlighting the trade-off between performance and power consumption, and suggesting the efficiency of MPPAs.	Martel et al. (2018)
	KPCA	Intra-node parallelization using multi-core CPUs and many-core GPUs are exploited to improve the parallel hierarchy of distributed-storage KPCA.	Xu et al. (2018)
	PCA	This work has explored the performance and energy efficiency of a common dimensionality reduction algorithm (PCA) for different HS image formats, i.e., data layouts in memory, (BSQ, BIP, BIL) using the embedded GPU included in NVIDIA's Jetson TX1.	Aragon et al. (2019)
	MSVM	Determined speed up in classification of different datasets when applying MSVM on low complexity real-time FPGA and software.	Gyaneshwar and Nidamanuri (2022)
Ground hyperspectral sensors	DR on FPGA	Used multiple algorithms for dimensionality reduction, image compression and anomaly detection.	Diaz et al. (2020)
	HW-LbL-FAD on FPGA	Achieved anomaly detection in hyperspectral images with a speed of 0.51 s/image using an FPGA.	Caba et al. (2022)
	Anomaly detection	Confirmed increase efficiency of GPU over CPU for anomaly detection in real-time with aerial hyperspectral data.	Tarabalka et al. (2009)
Pavia University and Indian Pines	Manifold learning	Implementation of these algorithms on CUDA based GPU architecture increased its performance.	Campana-Olivo and Manian (2011)
	gaPCA	Simple implementation of gaPCA algorithm on CPU, and GPU.	Machidon et al. (2020)
	KPCA	Hybrid of linear and nonlinear models can help reduce computational complexity.	Mohan and Venkatesan (2020)
	LPDBL on FPGA	The hyperspectral target detection based on the LPDBL algorithm was proposed. Due to its simple, excellent generalization ability, and quick processing of LPDBL, it was used for HSI target detection.	Shibi and Gayathri (2021)

(continued on next page)

Table 4 (*continued*)

Sensor name	Algorithm/ technique	Findings	Authors
	RFE and SFM	Identification of optimal wavelengths using multiple feature-selection methods in the scikit-learn ML library to detect peanut plants infected with *A. rolfsii* at various stages of disease development.	Wei et al. (2021)
	KMNF	GPU implementation achieves 60 times more speed.	Xue et al. (2021)
	Wavelet reduction	Achieved 90 % less speed in training CNN models using FPGA based parallel accelerator.	Baba and Bonny (2023)
–	pICA	High data transfer rate on FPGA	Du et al. (2004)

Note: The nomenclature should be referred for the abbreviations used.

Table 5
Accuracies of deep learning and machine learning models in agricultural applications.

Application	Features	Model	Accuracy	References
Basal Stem Rot	Band Subset (1)	VGG16	91.93 %	Yong et al. (2023)
Potato Late Blight	Full bands (204)	PLB-2D-3D-A (2D-3D CNN)	73.90 %	Qi et al. (2023)
	Band Subset (6)	PLB-2D-3D-A (2D-3D CNN)	79.00 %	
Coffee Beans Defect	Full bands (25)	2D-3D CNN	96.40 %	Chen et al. (2022)
	Band Subset (3)	2D-3D CNN	98.60 %	
Strawberry Ripeness	Band Subset (2)	AlexNet	98.60 %	Gao et al. (2020)
	Band Subset (2)	SVM	95.00 %	
Yellow Rust	Full Bands (125)	DCNN	85.00 %	Zhang et al., (2019a)
	Full Bands (125)	RF	77.00 %	
Charcoal rot	Full Bands (240)	3D-CNN	95.73 %	Nagasubramanian et al. (2019)
Orobanche cumana	Full Bands (162)	Logistic Regression	89.00 %	Atsmon et al. (2022)
	Band Subset (10)		82.00 %	
Weed and crops	Band Subset (10)	PLS-DA	86.20 %	Ahmed et al. (2022)

such as different crops or soil types (Khan et al., 2022). ML algorithms can also be used to perform regression analysis, making predictions about crop yields or disease severity based on hyperspectral data (Thomas et al., 2018). ML and statistical analysis techniques necessitate human input in the form of parameter selection by a subject matter expert, making them input-intensive methods (see Table 6).

DL algorithms, on the other hand, are more advanced than ML (Wang et al., 2021). DL consists of artificial neural networks with multiple hidden layers that allow for more complex data processing (Mishra et al., 2022a). DL algorithms are particularly well suited to tasks that involve complex relationships between inputs and outputs. For example, DL algorithms have been used to detect crop diseases by analyzing hyperspectral images and identifying spatial patterns in the data that correspond to different diseases (Passos and Mishra, 2022). The benefits of using ML and DL in the analysis of ground hyperspectral data in agriculture include improved accuracy in crop yield predictions, early detection of diseases and pests, the ability to monitor crop growth in real-time, and possible deployment of these models to robots and platforms. However, there are also some limitations to consider: ML and DL algorithms require large amounts of training data and complex algorithms that are difficult to interpret making it challenging to understand the underlying relationships between inputs and outputs. ML algorithms are simpler and easier to interpret but may not be as effective in processing complex relationships between inputs and outputs. DL algorithms are more complex and can process large amounts of data and identify complex relationships between inputs and outputs.

DL algorithms have emerged as a promising solution for HSI applications due to their automation capabilities, robustness, high accuracy, and scalability (Passos and Mishra, 2022; Xu et al., 2020). The automation of feature extraction and classification reduces the need for manual feature selection, speeding up the process (Fig. 9) (Wang et al., 2021). The robustness of these algorithms to noise and variations in the data makes them ideal applications where data quality can be an issue. The high accuracy of these algorithms, especially convolutional neural networks (CNNs), is due to their ability to learn complex patterns and features in large amounts of data. These algorithms can also be easily scaled to handle large amounts of data, and transfer learning can further enhance their scalability. Raw hyperspectral image dataset can be used to train the CNN model and, in many cases, has been reported to outperform traditional ML models (Qi et al., 2023).

4.4.1. Addressing the issue of system memory exhaustion for high-dimensional data

During DL training, large sizes of individual hyperspectral images can quickly exhaust the system memory even with a limited number of training samples. This is a major issue as DL models require a large number of training samples for proper model generalization. If the data size itself limits this, a considerable reduction in spatial resolution and spectral resolutions needs to be performed. Dimensionality reduction techniques work well for ML applications. However, for DL applications that use 3D data cubes as input, handling the data becomes even more challenging. These deep learning applications struggle to support very large datasets. Distributed learning or parallelism techniques are model training frameworks that allows distribution of data or model over multiple workers during training, these workers (systems) can be CPUs, GPUs, and TPUs (Gupta and Raskar, 2018). Using these frameworks multiple workers are utilized to conduct the model training. In data-distributed learning, a subset of input data is equally shared among the members and each member receives a copy of the replicated model. Whereas in model-distributed learning parts of the model are distributed to each worker and the data is replicated (Langer et al., 2020; Sergeev and Del Balso, 2018). Spatial parallelism works in a similar principle but instead of dividing the data or model as a whole it shards the spatial dimension of an individual image itself and shares it with available workers. This can allow the utilization of high spatial and spectral resolution hyperspectral images for DA training. Currently, spatial parallelism is only supported on Google's TPU infrastructure using a library called Mesh-Tensorflow (Shazeer et al., 2018). While application of spatial parallelism with agriculture hyperspectral data could not be found. A recent study utilized medical images of resolution $512 \times 512 \times 512$ to train a 3D Unet model (Hou et al., 2019). This is a promising area that will ensure more adaptability of hyperspectral data with state-of-the-art DL models.

4.4.2. Data augmentation of hyperspectral images

Data augmentation is a well-established technique for DL where mathematical operations (e.g., rotation, blur, shear, sharpen, brightness,

Table 6
Application of hyperspectral imaging in precision agriculture.

4	Subject	Sensor	Mode	Range (nm)		ML/DL	Study	Authors
Disease Detection & classification	Oil Palm	Cubert FireflEYE S185	Snapshot	890–950	L	DL: VGG16, RCNN	Detection of basal stem rot in oil palm.	Yong et al. (2023)
	Winter Wheat	ASD FieldSpec spectrometer	Point Scan	350–2500	L	ML: XGBoost	Study of XGBoost classifier with feature selection using correlation analysis random forest for vegetative indices, achieving 87.1 % overall accuracy.	Huang et al. (2022)
	Apples	Specim N17E	Line Scan	900–1700	L	ML: GTB	Codling Moth pest classification in Apples (91.6 % Acc) supervised model	Ekramirad et al. (2022)
	Potato	Specim FX10	Line Scan	400–1000	LF	ML: Logistic Regression	Lab vs Field detection model: difficulty in developing one model for both conditions (poor lab model performance on field data and poor field model performance on lab data)	Appeltans et al. (2022)
	Leek	Specim FX10	Line Scan	400–1000	LF	ML: Logistic Regression	Logistic regression supervised ML model was trained on field hyperspectral data. The model was not tested in real-time conditions.	Appeltans et al. (2021)
	Scindapsus aureus	Specim IQ (handheld)	Line Scan	400–1000	L	ML: SVM	A SVM classification model was used to detect defects in *Scindapsus aureus* leaves through the analysis of PCA-based spectral feature extraction in a laboratory setting.	Xiao and Wang (2020)
	Apple	PS-V10E SPECIM	Line Scan	356–1000	L	ML: DT, KNN, ensemble bagged, DT and weighted K nearest neighbor	Ensemble bagged supervised ML model was trained to classify apple disease.	Shuaibu et al. (2018)
	Apple	PS-V10E SPECIM	Line Scan	356–1018	L	DL: DNN, FCN	The paper presents the mRMR method, which is particularly useful for handling a vast number of options such as hyper-spectral images due to its lower computational complexity.	Park et al. (2018)
	Soybean Seeds	Headwall VNIR-A	Line Scan	400–1000	L	ML: TPE-RBF-SVM	Multi-class Soybean seed classifier (TPE-optimized RBF-SVM)	Zhao et al. (2022)
	grapevine	Specim Imspector V10E	Line Scan	380–1028	L	ML: PLS	Classification	Diago et al. (2013)
Crop Monitoring	Apple	ImSpector V10E	Line Scan	400–1000 and 1000–2500	L	ML: SVM, SLOG, SMO	Classification	Siedliska et al. (2014)
	Winter Wheat	FieldSpec4 spectrometer	Point Scan	350– 2500	L	ML: GBRT	Chlorophyll content prediction: BP NN and GB RT Model examined.	Wang et al. (2022)
	Wheat	ImSpector V10E-PS	Line Scan	360–1025	L	ML	Spectral and textural information fusion for successful image classification and crop monitoring (supervised and unsupervised ML)	Jiang et al. (2021)
	Rice	ImSpector N17E;	Line Scan	874–1734	L	ML: BPNN, RF, PLSR	Compared three feature selection method vegetation indices, model-based features, and PCA	Elsherbiny et al. (2021)
	Wheat and Maize	Cubert S185	Snapshot	450–950	F	ML: LM, BP, SVM, and RF	In lab analysis of Leaf chlorophyll content was estimated by linear regression, back propagation neural network, SVM	Zhu et al. (2020)
	Cotton, winter wheat, maize	ASD FieldSpec	Point Scan	350–2500	L	ML: ANN, SVMR, PLSR, PROSAIL	The findings showed that there was no one ideal	Nie et al. (2023)

(*continued on next page*)

Table 6 (*continued*)

4	Subject	Sensor	Mode	Range (nm)		ML/DL	Study	Authors
							model for accurately calculating the LAI of various crops because the correlation between specific hyperspectral reflectance and the LAI of different crops varied.	
	Strawberry	GaiaField-V10E	Snapshot	370–1015	L	ML: SVM, AlexNet CNN	Supervised classification study of strawberry ripeness done in lab.	Gao et al. (2020)
	Apple	SVC HR-1024i	Point Scan	360–2500	L	ML: PLSR	Classification	Jarolmasjed et al. (2018)
	Sesame oil	Specim ImSpectorV10E	Line Scan	325–1075			Comparison of various feature selection methods like SVM-MFFS, SPASVM, UVESVM	Deng et al. (2013)
Weed detection	Barnyard grass and Weedy rice in rice.	ImSpector V10E	Line Scan	380–1024	L	ML: Linear kernel based SVM	Leaf data was used to make the training data. This approch does not incorporate real-time data processing.	Zhang et al., (2019b)
	Corn vs Barnyard, Yellow nutsedge, Crab, Quack, Canada Thistle, Sow thistle, Lamb's Quarter, Redroot pigweed	CASI	Line Scan	409–947 nm	F	Statistics, DT, and Artificial Neural Network	Preferred DT over ANN even though ANN had better results. Due to DT's ability to form precise rules	Goel et al., (2003a); Goel et al., (2003b)
	Canola, Peas and Wheat Vs Redroot pigweed and Wild oat	prototype		400–1000 nm	F	NN and MLC	Determined that NN was a better classifier than MLC.	Eddy et al. (2006)
	Turfgrass Vs Dallisgrass, southern crabgrass, eclipta and Virginia buttonweed	–	Point Scan	350–2500 nm	G, F	ML/BSBC, SDA	ML/BSBC performed better than discriminant analysis. Classification results were better with field data as compared to greenhouse data.	Hutto et al. (2006)
	Sunflower Vs Ridolfia segetum	ASD FieldSpec	Point Scan	325–1075 nm	F	Statistical	Studied statistical difference between soil and different phenological stages of sunflower and R. segetum.	Peña-Barragán et al. (2006)
	Sugarbeet Vs Wild buckwheat, field horsetail, green foxtail, and common chickweed	ImSpector V10	Line Scan	400–1000 nm	F	Wavelet transformation, DA	Data compression was achieved using wavelet transformation and stepwise variable selection and statistical discriminant analysis performed better classification.	(Okamoto et al., 2007)
	Field pea, canola, spring wheat Vs Redroot pigweed and wild oat	Filter + CCD (Sony, ICX414AL)	Line Scan	400–1000 nm	F	MCARI, HS-ANN, MLC	Image background was removed from training images. Authors found HS-ANN to give better results and suggested it as more suitable for real-time application.	Eddy et al. (2008)
	Soybean Vs Goosefoot pigweed, small crabgrass, field horsetail, pearlwort	ImSpector V10	Line Scan	360–1010 nm	F	LDA, NN	NDVI was used to remove soil background. NN performed better than LDA and PCA gave better results than raw data. But raw data has faster processing	Suzuki et al. (2008)
	Winter Wheat Vs Wild oat and canary grass	ASD FieldSpec	Point Scan	325–1075 nm	F	SDA	Suggested complete phenological stage classification using 15 bands from Red, Green, Blue and NIR regions	Gómez-Casero et al. (2010)
	Tomato Vs Black nightshade, redroot pigweed	Photometrics CoolSNAP$_{cf}$	Line Scan	384–810 nm	L	SDA, PCA, CDA	A global calibration method was developed that achieved a 92.2 % classification rate and solved the temperature sensitivity problem in single temperature models.	Zhang and Slaughter (2011)

(*continued on next page*)

Table 6 (*continued*)

4	Subject	Sensor	Mode	Range (nm)		ML/DL	Study	Authors
	Tomato Vs Black nightshade, redroot pigweed	Photometrics CoolSNAP$_{cf}$	Line Scan	400–795 nm	F	CBD	A study conducted over three seasons investigated the effects of seasonal variability in environmental conditions.	Zhang et al., (2012a)
	Annual ragweed, mugwort	ImSpector V10E	Line Scan	100–1000 nm	L	Statistical	Determined that 550 nm and 650 nm gave class separability between ragweed and mugwort	Dammer et al. (2013)
	Wheat Vs Broad leaf and grass weed	ImSpector V10E	Line Scan	300–1000 nm	F	PLS-DA	Six PLS-DA models were trained. Classification included sunlit and shaded areas of images along with soil.	Herrmann et al. (2013)
	Pine Vs Bugweed	AISA	Line Scan	400–900 nm	F#	SVM	SVM-RFE was used for feature selection and obtained 90 % accuracy in classifying aerial images of Bugweed patches in pine forests.	Atkinson et al. (2014)
	Field pea, spring wheat, canola Vs Wild oats, redroot pigweed	Filter + CCD (Sony, ICX414AL)	Line Scan	400–1000 nm	F	ANN, PCA, SDA	Study show that reduced band set (7 bands) achieved ANN classification result that was similar to the full band set data (61 bands)	Eddy et al. (2014)
	Palmer amaranth (resistant vs susceptible)	Resonon Pika II	Line Scan	394.3–896.917 nm	G, F	FLDA, Maximum Likelihood	14 bands out of 240 bands were used and achieved an accuracy of 93.5 %. They found higher reflectance in visible regions for susceptible plants and infrared regions for resistant plants.	Reddy et al. (2014)
	Cabbages Vs Barnard grass, small pigweed, goosegrass, crabgrass, and green foxtail	SWIR-N25E	Line Scan	1000–2500 nm	L	SAM	Pixel wise classification using ENVI and HSI analyzer. Applied preprocessing steps. This study is an example of high data curations.	Wei et al. (2015)
	Soybean Vs Non-glyphosate resistant redroot pigweed, Palmer amaranth	FieldSpec 3	Point Scan	350–2500 nm	G	RF	Random forest binary classifiers were trained to classify soybeans against weeds.	Fletcher and Reddy (2016)
	Maize Vs Creeping buttercup, Creeping thistle, charlock, chickweed, common dandelion, annual bluegrass, redshank, common nettle, common yellow woodsorrel and black medic	Inspector V9	Line Scan	435–834 nm	F	SOM, MOG, SVM, AE-NN	One class classifier was trained on pixel data.	Pantazi et al. (2016)

L: Lab, F: Field, ML: Machine Learning, DL: Deep Learning, #Airborne. The nomenclature should be referred for the additional abbreviations.

contrast, mirror) are applied to the data, tuning them slightly to increase the number of training samples. Hyperspectral data collection is labor and time-intensive, often resulting in limited training samples. Increasing the number of training samples helps the model to better generalize in classification tasks. Online and offline modes of data augmentation can be currently found in the literature. In online mode the augmentation is applied to the data during the training of models and in offline mode data is augmented and saved before the training (Nalepa et al., 2019; Rochac et al., 2019). Further, augmentations itself can be divided into two categories, (1) model-based augmentation, and (2) spatial transformation-based augmentation. Model-based augmentation uses DL models to create new variations of data. Generative adversarial network (GANs) utilizes the generator and discriminator blocks to generate new data from a given input data. The generator creates synthetic data to mimic real data, aiming to fool the discriminator. The discriminator, receiving both real and synthetic data, is trained to distinguish between them. Misclassifications are penalized, leading to the generator improving its data realism over time. There have been multiple variants of GANs, out of which deep convolutional generative adversarial networks (DCGANs) are mostly utilized in HSI (Tan et al., 2024). While CNNs support 3D and 1D data, current applications utilize DCGAN for 1D spectral data and have been reported to grain approximately a 10 % increase in classification results (Zhang et al., 2022). DCGANs are also utilized with ML models like DT, RF, and SVM (Tan et al., 2024). Spatial transformation-based data augmentations include rotate, flip, transpose, random occlusion, and zoom (Fig. 8). These methods can be applied to the data in an online or offline mode. Data augmentations, whether model-based or spatial transformation-based methods have proven results of helping the model in better generalization and classification accuracy (Haut et al., 2019).

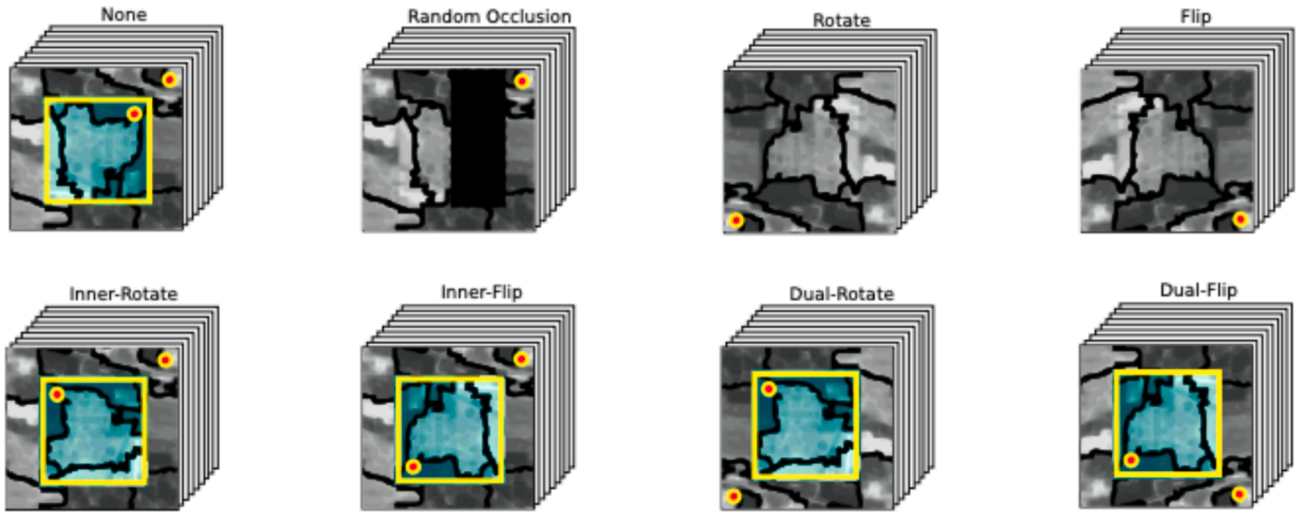

Fig. 8. Examples of various spatial transformation-based data augmentation techniques applied to hyperspectral images. The red marks depict the change in orientation from the original data (Acción et al., 2020). (For interpretation of the references to color in this figure legend, the reader is referred to the web version of this article.)

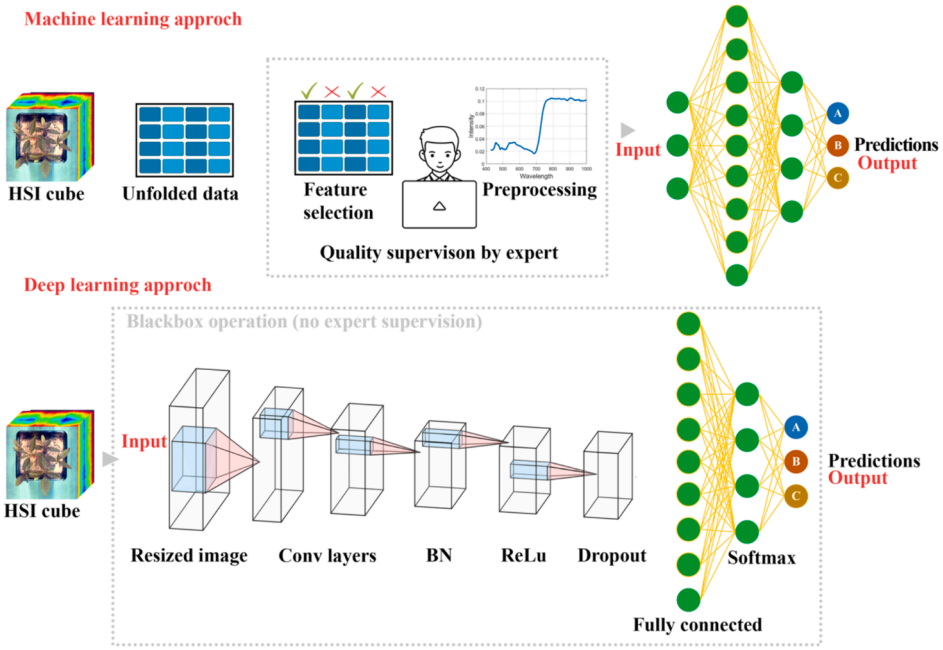

Fig. 9. A simplified illustration of a very basic 3D-CNN architecture.

5. Applications of hyperspectral in precision agriculture

5.1. Weed identification or classification studies

As weeds look spatially similar to crops, especially at an early stage. Implementation of HSI for weed identification is seen as a possible solution for the early detection of weeds. For proper weed management, the fields must be relieved of weed population before they take growth advantage over the crops. While with RGB images the trained models mostly rely on the spatial or textural features of objects to draw their inferences. The problem of differentiating between objects of similar color and texture can be solved with high spectral resolution data captured with hyperspectral sensors (Dammer et al., 2013; Okamoto et al., 2007). Due to this hyperspectral data can also be used to differentiate between biotypes of the same plant. Such as glyphosate-resistant and susceptible Palmer amaranth, which has been found to differ in reflection near the VNIR region (Reddy et al., 2014). Pure spectral signatures collected using point spectrometers in the VNIR region can classify different weeds like kochia, lamb's quarters, and waterhemp (Shirzadifar et al., 2018). Weeds are known to produce a very large number of seeds and grow herbicide resistant over time. Hyperspectral data studies have found better accuracy in differentiating germinating and non-germinating seeds and observed a strong correlation between physiological properties and herbicide response of Palmer amaranth using hyperspectral data. Which has been impossible with models trained on RGB images (Matzrafi et al., 2017). Portable hyperspectral sensors have the advantage of high spatial resolution. Studies that use airborne sensors often are useful to determine weed patches instead of individual weed crops (Atkinson et al., 2014). Using airborne sensors such as the Airborne Imaging Spectrometer for Applications (AISA) detection of small weed patches attains a low success rate due to low spatial resolution. However, the models excel on weed patches spread on

a higher surface area (Peerbhay et al., 2016). Thereby suggesting the increased efficiency of ground and UAV-mounted hyperspectral sensors in comparison to aircraft-mounted or satellite-mounted sensors in the context of spatial resolution.

Various ML methods are used to train supervised classification models to classify weeds from crops. Irrespective of the mode of data collection. This data is unfolded and preprocessed (Ahmed et al., 2022). ML model classification is therefore highly offline and requires intense knowledge of the data. Due to this offline nature, ML analysis is often recommended for investigation wavelength interaction with a material.

DL utilizes spatial and spectral information from hyperspectral data thereby keeping information generally lost due to unfolding. DL models learn from multiple hidden layers that replicate neurons in the human brain. These layers work in a "black box" manner i.e., the models' learning parameters used to draw inferences are unknown. Multiple implementations of CNN models are seen in the literature. Authors have reported increased weed classification accuracies with fused 2D and 3D CNN models (Farooq et al., 2019). The 3D CNN-based networks such as the BS-Net FC are also used for feature selection and are reported to have increased accuracy compared to ML feature selection methods. DL models require a large amount of data for training and that demand is fulfilled using data augmentation (Diao et al., 2022).

Various platforms are developed utilizing HSI for weed identification. Custom fabricated sensor modules that record only the required significant wavelengths thereby reducing data and computational complexity at the first step itself are being used, these sensors are often supported by independently designed circuit boards or FPGAs and have been able to achieve near real-time speeds in weed identification (Symonds et al., 2015). Some platforms only focus on data collection without actuation tasks. One class of weed and crop classifiers trained on data collected using autonomously driven platforms has been reported to give good accuracy results (Pantazi et al., 2016). Multiclass models for weed identification are also developed which are trained data collected using platforms (Ahmed et al., 2022). Only a handful number of studies build platforms that can achieve analysis and actuations in real-time. Zhang et al. (2012a) conducted a two-part study of the identification of weeds and application of heated oil as a solution in row crops infested with weeds was able to achieve a ground speed of 0.04 m/s using a Bayesian classifier trained on 13 wavelengths in the range of 384–810 nm.

5.2. Detection of disease and pest

Plant growth can be adversely affected by disease, stress, and pest infestations, which can result in reduced yield and quality or even complete growth cessation. The VNIR region has been useful in detecting white tip disease and *Orobanche cumana* parasitism in sunflower plants (Atsmon et al., 2022). Logistic regression models trained on hyperspectral data can be used to classify plant health and different stages of disease damage at pre-symptomatic stage (Appeltans et al., 2021). Plant stress due to the presence of heavy metals like Hg has been detected using the NIR regions (Yu et al., 2021). The requirement for background removal and selection of diseased ROIs to improve the data quality is essential for some applications where the disease affected area is considerably smaller and surrounded by other areas. Such as the charcoal rot disease in soybean stems (Nagasubramanian et al., 2019). Spectral domain studies also apply various vegetation indices to determine the correlation of diseases with plant growth (Xue et al., 2023). Some implementations of 3D-CNN models have also used complete spectral bands as training input. This removes the need for the time-consuming feature selection step. Handheld hyperspectral sensors like the Specim IQ are available that have made data collection using the line scan method easy. DCNN models trained on data captured using UAVs have rendered good detection results for yellow rust disease in winter wheat (Zhang et al., 2019a). While DL has been proven to remove some intermediate analysis steps. Studies mentioned above do not apply trained models for real-time applications and focus on training models that are (1) able to accurately classify/detect subjects, and (2) reduce some preprocessing steps. While real-time applications of hyperspectral in disease and pest detection are limited. It is not debatable that real-time defect detection and actuation require low spectral bands to accommodate the processing and data transfer needs. DL provides the real-time speeds for such applications. Variations of CNN models like the fused 2D-3DCNN models have achieved analysis speeds of 0.03 s/image in inspecting 32 coffee beans in a single image and sorting them with a robotic arm (Chen et al., 2022).

5.3. Biochemical and biophysical analysis

Phenotyping and estimation of plant health can be determined by key factors such as leaf area index, chlorophyll and nitrogen content, crop yield, and water content. HSI using spectroscopy has proven to be more effective in detecting the impact of these parameters compared to multispectral and thermal imaging (Jarolmasjed et al., 2018). Water content is an important parameters for plants' health and freshness. A wavelength range of 1350–1650 nm has been found to successfully determine relative water content from hyperspectral data collected in field and laboratory conditions (Junttila et al., 2022). Preprocessing steps for hyperspectral data are important. Using raw spectral data for training ML models reduces accuracy in determining biochemical and biophysical parameters (Singh et al., 2022). Accurate fertilization planning for trees requires the quantification of nitrogen (N), as it is the primary limiting factor after water. Partial least square regression (PLSR) and vegetation indices have been used to determine nitrogen content in plants and physiological changes during daytime and drought conditions (Mertens et al., 2021; Rubio-Delgado et al., 2021). Exploration of the biochemical properties of plants generally depends on spectral data over spatial data. Studies that determine water content, nitrogen content or plant stress often use point scan spectrometers due to their high spectral resolution. Another reason for this is that biochemical factors do not necessarily depend on plants' physical parameters but their chemical composition. Hyperspectral platforms include the phenotyping platform called Phenovision (VIB-UGent Center for Plant Systems Biology, Ghent, Belgium) which facilitates automated temporal data collection using multiple sensors. Two of which are line scan hyperspectral sensors (ImSpector V10E and N25E) that provide a combined spectral range of 400–2500 nm. Vigneau et al. (2011) used a line scan sensor (HySpex VNIR 1600–160) mounted 1 m above the foliage on a linear rail mounted on a tractor with a spectral range of 400–1000 nm. No steps were taken to introduce artificial lighting sources as is normally observed and data was collected using sun irradiance. The plants captured were isolated by human intervention so that there was no occluding of leaves.

6. Applicability of hyperspectral imaging in precision agriculture

Implementation of multidimensional data in real-time systems is a multifaceted challenge. The ever-evolving fields of computer science and artificial intelligence are making it possible to work with high-dimensional data at comparable real-time speeds. However, in most current research, this is accomplished only after dimensionality reduction. As a result, the efficacy of utilizing HSI in contrast to RGB or multispectral images can be scrutinized. HSI has proven successful in scenarios where RGB imaging has been ineffective. As such, HSI has a distinct set of applications compared to RGB imaging. The applicability of HSI data, HSI platforms, and related advanced analysis and models are discussed subsequently.

6.1. Justification for using hyperspectral over RGB and multispectral data

Hyperspectral data is valuable due to its ability to conduct

spectroscopic analysis of materials. This enables the identification of biochemical plant traits, as well as the detection of disease and damage in plants, even when not visually apparent. Therefore primarily, HSI is an investigative tool that allows for the determination of valuable information about materials through the identification of significant features, typically limited to 5–10 bands. After identifying the significant investigative plant traits using the complete spectral bands, it is logical to select sensors that operate within those significant bands, considering the requirements for real-time data acquisition.

6.2. Hyperspectral platforms

Current hyperspectral platforms can be classified into two distinct categories: those designed exclusively for data collection, and those that incorporate actuation tasks in conjunction with data collection. Data collection using point scan sensors is typically performed manually and with the aid of handheld or backpack devices. Mobile data collection platforms are restricted to the use of line scan or snapshot sensors, with no studies found utilizing point scan sensors. While no significant difference in the accuracies of statistical or ML models was observed between closed systems, using artificial illumination sources and open systems that utilize solar irradiance as an illumination source, it should be noted that open system platforms are dependent on solar irradiance for data collection and no data was reportedly collected during cloudy or nighttime conditions. Current platforms that perform actuation tasks implement significant dimensionality reduction techniques to achieve real-time processing speeds. This is justifiable, as high-dimensional spectral data is not required to achieve satisfactory model accuracies. In the context of PA, HSI can be used to identify significant bands, enabling the development of real-time platforms instead equipped with multispectral or CCD sensors with variable filters within the range of these significant bands. In cases where spatial and spectral differences are minimal, the use of hyperspectral sensors is justified, particularly when low-band sensors in the specific wavelength region are unavailable or when a tool is being developed for multiple objects with varying spatial and spectral profiles.

6.3. Machine learning and deep learning

ML technologies have facilitated the development of classification models capable of achieving high accuracy in detecting various plant traits. The incorporation of spatial information with spectral data has been made possible through DL. Despite their high accuracy, these models still rely on data preprocessing and augmentation. While it can be argued that DL requires less preprocessing than traditional ML models, it necessitates a large dataset, which can be challenging to obtain in the case of HSI compared to RGB images. While research on training these models is on the rise, it is important to also focus on their deployment, which is currently receiving less attention.

7. Overall observation on real-time application of hyperspectral imaging

HSI has demonstrated superior results in various agricultural applications discussed in this review. The high dimensionality of hyperspectral data allows it to solve problems that are not achievable with RGB and multispectral imaging. Specifically, its ability to determine the interaction of different objects in a wide wavelength range. This investigation can help us find dissimilarities between objects of the same textural, color, and physical properties, thereby differentiating objects based on their chemical composition. For example, differentiating among biotypes of the same plant, classifying crops and weeds that look similar, and finding defects in fruits that are not visible to the naked eye. Some of the significant conclusions obtained from this review are listed below:

1. Dimensionality reduction is a major step, found common in most studies. The selection of the most significant bands helps reduce data size, remove data redundancy, and help in real-time applications.
2. The wavelength range of 400–1000 nm is the most common range for agricultural applications. Whereas the significant wavelength for different applications differs.
3. The choice of preprocessing steps solely depends on the researcher and the models' accuracy. There is no fixed set of rules for the selection of preprocessing steps. The most common preprocessing steps found were image calibration and scatter correction.
4. Implementation of FPGA and GPUs in the analysis pipeline can improve processing speeds. FPGA, due to their ability to build custom logic, have been known to have slightly higher speeds when compared to GPUs and CPUs. FPGA also allows the implementation of data compression logic, giving an overall better performance. The implementation of FPGAs is currently lacking in general due to limited knowledge, especially in the agricultural community.
5. DL models compared to ML models allow for a more streamlined analysis approach. ML models are highly preprocessing dependent. Whereas DL models do not require intense or sometimes perform without preprocessing.
6. Data augmentation is a beneficial approach for the training of DL models and increasing the models' generalization capabilities with limited hyperspectral data captured.
7. System memory exhaustion issues commonly seen with training high-resolution hyperspectral images can be solved with distributed learning frameworks.
8. Explanation of biochemical plant traits is usually achieved using spectral data exploitation without the need for spatial information. This is currently processed with the help of ML models or 1D-CNN models. But fused models like 2D-3D CNN have been found to be giving increased accuracies recently.
9. Agricultural research currently developing hyperspectral platforms is increasing. This trend is predicted to grow in the coming years as technology advances.

8. Future research directions

The current research trend in HSI and PA has comprehensively demonstrated that a shift towards real-time applications is taking place. However, technology and analysis are in the initial stages of development, and for this scientific field and related industry to grow more research and development is required. Based on this review, some of the potential future research directions are: (i) Development of open-source software, libraries, and toolboxes for hyperspectral data acquisition. Such tools should support UAV- and UGV-mounted sensors compatible with embedded systems like the NVIDIA Jetsons or other powerful portable platforms. (ii) Development of cost-effective and practical real-time hyperspectral data recording platforms is a crucial area for future research and development. (iii) Increased research on the applications of FPGAs and GPUs in hyperspectral data analysis for PA. More importantly, FPGAs have not been utilized by the agricultural community as thoroughly as CPUs and GPUs. (iv) Deployment of ML and DL models for HSI real-time PA applications. Even though many models are trained with good accuracy, only a few are currently deployed, and large-scale consolidation of models that make the model rugged and applicable to several scenarios should be studied. (v) Fabrication and deployment of autonomous platforms that use independently developed tools for data acquisition, navigation, analysis, and model deployment is another critical area of future research.

9. Conclusions

A systematic analysis of literature from the past 20 years (2003–2023) reveals the significant potential of HSI in PA through real-time crop monitoring and analysis. The following systematic literature

review methodology revealed a growing trend towards the utilization of high spatial resolution hyperspectral sensors in agricultural applications. Recent research efforts have focused on spectral analysis with the development of platforms for data collection, analysis, and actuation tasks. Studies have employed ground vehicles, UAVs, and UGVs as platforms for both field and laboratory applications. Some researchers suggest the potential for real-time applications in the future, and several studies have already demonstrated the successful real-time application of hyperspectral sensors. Both natural solar in the fields and halogen lighting in closed systems are illumination sources used for these platforms. The choice of illumination did not affect model accuracies, but it did impact data recording conditions and introduce variability in lighting and processing difficulties.

Only a limited number of open-source software options were available for data acquisition and analysis, with most studies relying on proprietary software. Signal correction was identified as a crucial preprocessing step while utilizing ML models and statistical analysis. Background removal or segmentation techniques were employed to spatial-spectral images to isolate pure spectra of different classes. Research on data compression for ground hyperspectral sensors is still in its early stages, with most work being conducted on satellite hyperspectral data. Dimensionality reduction was identified as the most common approach to reducing data size, with a trend toward selecting 10 or fewer bands from the entire spectral range for efficient and real-time processing speeds. There is a growing trend toward the utilization of GPUs and embedded systems in hyperspectral data analysis. The implementation of FPGAs has primarily been limited to airborne or satellite sensors, but their use with ground-based sensors is beginning to emerge. Only a limited number of ground-based hyperspectral data recording platforms, despite numerous advantages, can perform real-time analysis, and are primarily restricted to laboratory use.

Recent research trends have demonstrated the potential of DL algorithms as a powerful tool in comparison to conventional ML techniques, as they can alleviate the burden of feature selection and preprocessing to some extent. Comparison between DL and ML models using full, and subset of spectral dimension did not affect the accuracies. The increasing research trend in this field shows more applications begin to employ 3D hyperspectral data (with spatial and spectral information) as training samples for DL training. Model or spatial transformation-based data augmentations have helped alleviate the problem of limited hyperspectral data. Distributed training frameworks can help training of high-resolution hyperspectral images for DL. Data acquisition, preprocessing, and dimensionality reduction methods are significant for real-time applications. The application of HSI in PA is primarily focused on classification tasks using ML and DL models. Key research areas of interest include the identification of weeds, diseases, and pests, as well as the analysis of biochemical and biophysical plant traits. Studies have also explored the identification of significant spectral bands for specific applications, but the findings have not been consistently supported by follow-up studies. Overall, the NIR range of 400–1000 nm is widely accepted as the most relevant for agricultural applications.

While most studies have used conventional data acquisition and processing with proprietary software, only limited studies explored the use of embedded systems, FPGAs, GPUs, and analysis designed specifically for real-time applications. Potential future research areas identified for the development of HSI in PA include software and cost-effective hardware development, FPGAs and GPUs usage, consolidated ML and DL models, and the development of autonomous platforms. Overall, this review highlights the immense potential of ground-based HSI in PA and its future as an investigative tool for real-time crop monitoring and analysis. The advancement of HSI technology holds tremendous promise for the future of PA and food security.

CRediT authorship contribution statement

Billy G. Ram: . **Peter Oduor:** Writing – review & editing. **C. Igathinathane:** Writing – review & editing. **Kirk Howatt:** Methodology, Resources. **Xin Sun:** Funding acquisition, Methodology, Resources, Supervision, Writing – review & editing.

Declaration of competing interest

The authors declare that they have no known competing financial interests or personal relationships that could have appeared to influence the work reported in this paper.

Data availability

No data was used for the research described in the article.

Acknowledgements

This review study is based upon work partially supported by the U.S. Department of Agriculture, agreement number 58-6064-8-023. Any opinions, finding, conclusions or recommendations expressed in this publication are those of the author(s) and do not necessarily reflect the view of the U.S. Department of Agriculture (USDA). This work is/was supported by the USDA National Institute of Food and Agriculture, Hatch project numbers ND01487 and ND01493.

References

Acción, Á., Argüello, F., Heras, D.B., 2020. Dual-window superpixel data augmentation for hyperspectral image classification. Appl. Sci. https://doi.org/10.3390/app10248833.

Adão, T., Hruska, J., Pádua, L., Bessa, J., Peres, E., Morais, R., Sousa, J., 2017. Hyperspectral imaging: A review on UAV-based sensors, data processing and applications for agriculture and forestry. Remote. Sens. 9, 1110. https://doi.org/10.3390/rs9111110.

Ahmed, M.R., Ram, B.G., Koparan, C., Howatt, K., Zhang, Y., Sun, X., 2022. Multiclass classification on soybean and weed species using a novel customized greenhouse robotic and hyperspectral combination system. Available at SSRN 4044574. DOI: 10.2139/ssrn.4044574.

Ali, M.M., Bachik, N.A., Muhadi, N.A., Tuan Yusof, T.N., Gomes, C., 2019. Non-destructive techniques of detecting plant diseases: A review. Physiol. Mol. Plant Pathol. 108, 101426 https://doi.org/10.1016/j.pmpp.2019.101426.

Altamimi, A., Ben Youssef, B., 2022. A systematic review of hardware-accelerated compression of remotely sensed hyperspectral images. Sensors 22 (1), 263. https://doi.org/10.3390/s22010263.

Anastasiou, E., Balafoutis, A., Darra, N., Psiroukis, V., Biniari, A., Xanthopoulos, G., Fountas, S., 2018. Satellite and proximal sensing to estimate the yield and quality of table grapes. Agriculture 8 (7), 94. https://www.mdpi.com/2077-0472/8/7/94.

Appeltans, S., Pieters, J.G., Mouazen, A.M., 2021. Detection of leek white tip disease under field conditions using hyperspectral proximal sensing and supervised machine learning. Comput. Electron. Agric. 190, 106453 https://doi.org/10.1016/j.compag.2021.106453.

Appeltans, S., Pieters, J., Mouazen, A., 2022. Potential of laboratory hyperspectral data for in-field detection of phytophthora infestans on potato. Precis. Agric. 23 (3), 876–893. https://doi.org/10.1007/s11119-021-09865-0.

Aragon, J.S., Ramirez, S.S., Lopez, R.L., Quintin, D.M., Perea, R.S., Martinez, E.J., Alvaro, C.S., 2019. Characterizing hyperspectral data layouts: Performance and energy efficiency in embedded GPUs for PCA-based dimensionality reduction. 34th Conference on Design of Circuits and Integrated Systems (DCIS). DOI: 10.1109/DCIS201949030.2019.8959835.

Atkinson, J.T., Ismail, R., Robertson, M., 2014. Mapping bugweed (solanum mauritianum) infestations in pinus patula plantations using hyperspectral imagery and support vector machines. IEEE J. Sel. Top. Appl. Earth Obs. Remote Sens. 7 (1), 17–28. https://doi.org/10.1109/JSTARS.2013.2257988.

Atsmon, G., Nehurai, O., Kizel, F., Eizenberg, H., Nisim Lati, R., 2022. Hyperspectral imaging facilitates early detection of orobanche cumana below-ground parasitism on sunflower under field conditions. Comput. Electron. Agric. 196, 106881 https://doi.org/10.1016/j.compag.2022.106881.

Baba, A., Bonny, T., 2023. FPGA-based parallel implementation to classify hyperspectral images by using a convolutional neural network. Integration 92, 15–23. https://doi.org/10.1016/j.vlsi.2023.04.003.

Barbedo, J.G.A., 2023. A review on the combination of deep learning techniques with proximal hyperspectral images in agriculture. Comput. Electron. Agric. 210, 107920 https://doi.org/10.1016/j.compag.2023.107920.

Barrios Alfaro, Y., Rodríguez, A., Sánchez Clemente, A.J., Pérez, A., López, S., Otero, A., de la Torre, E., Sarmiento, R., 2020. Lossy hyperspectral image compression on a reconfigurable and fault-tolerant FPGA-based adaptive computing platform. Electronics 9 (10), 1576. https://doi.org/10.3390/electronics9101576.

Bellman, R.E., 1957. Dynamic programming, ser. Cambridge Studies in Speech Science and Communication. Princeton University Press, Princeton.

Benelli, A., Cevoli, C., Fabbri, A., 2020. In-field hyperspectral imaging: An overview on the ground-based applications in agriculture. J. Agric. Eng. 51 (3), 129–139. https://doi.org/10.4081/jae.2020.1030.

Berger, K., Machwitz, M., Kycko, M., Kefauver, S.C., Van Wittenberghe, S., Gerhards, M., Verrelst, J., Atzberger, C., van der Tol, C., Damm, A., Rascher, U., Herrmann, I., Paz, V.S., Fahrner, S., Pieruschka, R., Prikaziuk, E., Buchaillot, M.L., Halabuk, A., Celesti, M., Koren, G., Gormus, E.T., Rossini, M., Foerster, M., Siegmann, B., Abdelbaki, A., Tagliabue, G., Hank, T., Darvishzadeh, R., Aasen, H., Garcia, M., Pôças, I., Bandopadhyay, S., Sulis, M., Tomelleri, E., Rozenstein, O., Filchev, L., Stancile, G., Schlerf, M., 2022. Multi-sensor spectral synergies for crop stress detection and monitoring in the optical domain: A review. Remote Sens. Environ. 280, 113198 https://doi.org/10.1016/j.rse.2022.113198.

Bouguettaya, A., Zarzour, H., Kechida, A., Taberkit, A.M., 2022. Deep learning techniques to classify agricultural crops through UAV imagery: A review. Neural. Comput. Appl. 34 (12), 9511–9536. https://doi.org/10.1007/s00521-022-07104-9.

Caba, J., Díaz, M., Barba, J., Guerra, R., Escolar, S., López, S., 2022. Low-power hyperspectral anomaly detector implementation in cost-optimized FPGA devices. IEEE J. Sel. Top. Appl. Earth Obs. Remote Sens. 15, 2379–2393. https://doi.org/10.1109/JSTARS.2022.3157740.

Campana-Olivo, R., Manian, V., 2011. Parallel implementation of nonlinear dimensionality reduction methods applied in object segmentation using CUDA in GPU. Conference on Algorithms and Technologies for Multispectral, Hyperspectral, and Ultraspectral Imagery XVII. https://doi.org/10.1117/12.884767.

Chen, S.-Y., Chiu, M.-F., Zou, X.-W., 2022. Real-time defect inspection of green coffee beans using NIR snapshot hyperspectral imaging. Comput. Electron. Agric. 197 https://doi.org/10.1016/j.compag.2022.106970.

Corti, M., Gallina, P.M., Cavalli, D., Cabassi, G., 2017. Hyperspectral imaging of spinach canopy under combined water and nitrogen stress to estimate biomass, water, and nitrogen content. Biosys. Eng. 158, 38–50. https://doi.org/10.1016/j.biosystemseng.2017.03.006.

Corti, M., Cavalli, D., Cabassi, G., Marino Gallina, P., Bechini, L., 2018. Does remote and proximal optical sensing successfully estimate maize variables? A review. Eur. J. Agron. 99, 37–50. https://doi.org/10.1016/j.eja.2018.06.008.

Dammer, K.-H., Intress, J., Beuche, H., Selbeck, J., Dworak, V., 2013. Discrimination of ambrosia artemisiifolia and artemisia vulgaris by hyperspectral image analysis during the growing season. Weed Res. 53 (2), 146–156. https://doi.org/10.1111/wre.12006.

Deng, L., Sun, J., Chen, Y., Lu, H., Duan, F.Z., Zhu, L., Fan, T.X., 2021. M2h-net: A reconstruction method for hyperspectral remotely sensed imagery. ISPRS J. Photogramm. Remote Sens. 173, 323–348. https://doi.org/10.1016/j.isprsjprs.2021.01.019.

Deng, S., Xu, Y., Li, L., Li, X., He, Y., 2013. A feature-selection algorithm based on support vector machine-multiclass for hyperspectral visible spectral analysis. J. Food Eng. 119 (1), 159–166. https://doi.org/10.1016/j.jfoodeng.2013.05.024.

Diago, M.P., Fernandes, A.M., Millan, B., Tardáguila, J., Melo-Pinto, P., 2013. Identification of grapevine varieties using leaf spectroscopy and partial least squares. Comput. Electron. Agric. 99, 7–13. https://doi.org/10.1016/j.compag.2013.08.021.

Diao, Z., Yan, J., He, Z., Zhao, S., Guo, P., 2022. Corn seedling recognition algorithm based on hyperspectral image and lightweight 3D-CNN. Comput. Electron. Agric. 201, 107343 https://doi.org/10.1016/j.compag.2022.107343.

Diaz, M., Guerra, R., Horstrand, P., Lopez, S., Lopez, J.F., Sarmiento, R., (2020). Towards the concurrent execution of multiple hyperspectral imaging applications by means of computationally simple operations. Remote Sens., 12(8), Article 1343. DOI: 10.3390/rs12081343.

Díaz, M., Guerra, R., Horstrand, P., Martel, E., López, S., López, J.F., Sarmiento, R., 2019. Real-time hyperspectral image compression onto embedded GPUs. IEEE J. Sel. Top. Appl. Earth Obs. Remote Sens. 12 (8), 2792–2809. https://doi.org/10.1109/JSTARS.2019.2917088.

Du, H.T., Qi, H.R., ieee, (2004). An FPGA implementation of parallel ICA for dimensionality reduction in hyperspectral images. IEEE International Geoscience and Remote Sensing Symposium. 3257-3260. DOI: 10.1109/IGARSS.2004.1370396.

Dua, Y., Kumar, V., Singh, R.S., 2020. Comprehensive review of hyperspectral image compression algorithms, 090902 OptEn 59 (9). https://doi.org/10.1117/1.OE.59.9.090902.

Eddy, P., Smith, A., Hill, B., Peddle, D., Coburn, C., Blackshaw, R., 2006. Comparison of neural network and maximum likelihood high resolution image classification for weed detection in crops: Applications in precision agriculture. IEEE International Symposium on Geoscience and Remote Sensing. 2006, 116–119. https://doi.org/10.1109/IGARSS.2006.35.

Eddy, P., Smith, A., Hill, B., Peddle, D., Coburn, C., Blackshaw, R., 2008. Hybrid segmentation–artificial neural network classification of high resolution hyperspectral imagery for site-specific herbicide management in agriculture. PE&RS 74 (10), 1249–1257. https://doi.org/10.14358/PERS.74.10.1249.

Eddy, P.R., Smith, A.M., Hill, B.D., Peddle, D.R., Coburn, C.A., Blackshaw, R.E., 2014. Weed and crop discrimination using hyperspectral image data and reduced bandsets. CaJRS 39 (6), 481–490. https://doi.org/10.5589/m14-001.

Edelman, G.J., Gaston, E., van Leeuwen, T.G., Cullen, P.J., Aalders, M.C.G., 2012. Hyperspectral imaging for non-contact analysis of forensic traces. Forensic Sci. Int. 223 (1), 28–39. https://doi.org/10.1016/j.forsciint.2012.09.012.

Eh Teet, S., Hashim, N., 2023. Recent advances of application of optical imaging techniques for disease detection in fruits and vegetables: A review. Food Control 152, 109849. https://doi.org/10.1016/j.foodcont.2023.109849.

Ekramirad, N., Khaled, A.Y., Doyle, L.E., Loeb, J.R., Donohue, K.D., Villanueva, R.T., Adedeji, A.A., 2022. Nondestructive detection of codling moth infestation in apples using pixel-based nir hyperspectral imaging with machine learning and feature selection. Foods 11 (1), 8. https://doi.org/10.3390/foods11010008.

Elsherbiny, O., Fan, Y., Zhou, L., Qiu, Z., 2021. Fusion of feature selection methods and regression algorithms for predicting the canopy water content of rice based on hyperspectral data. Agriculture 11 (1), 51. https://doi.org/10.3390/agriculture11010051.

Fahlgren, N., Feldman, M., Gehan, M.A., Wilson, M.S., Shyu, C., Bryant, D.W., Hill, S.T., McEntee, C.J., Warnasooriya, S.N., Kumar, I., Ficor, T., Turnipseed, S., Gilbert, K.B., Brutnell, T.P., Carrington, J.C., Mockler, T.C., Baxter, I., 2015. A versatile phenotyping system and analytics platform reveals diverse temporal responses to water availability in setaria. Mol. Plant 8 (10), 1520–1535. https://doi.org/10.1016/j.molp.2015.06.005.

Fang, M.Q., Fang, J.B., Zhang, W.M., 2017. Efficient and portable parallel framework for hyperspectral image dimensionality reduction on heterogeneous platforms. J. Appl. Remote Sens. 11, 015022 https://doi.org/10.1117/1.Jrs.11.015022.

Farooq, A., Jia, X., Hu, J., Zhou, J., 2019. Multi-resolution weed classification via convolutional neural network and superpixel based local binary pattern using remote sensing images. Remote Sens. 11 (14), 1692. https://www.mdpi.com/2072-4292/11/14/1692.

Fenzandez, D., Gonzalez, C., Mozos, D., Ieee, 2016. Dimensionality reduction of hyperspectral images using reconfigurable hardware. 26th International Conference on Field-Programmable Logic and Applications (FPL). DOI: 10.1109/fpl.2016.7577394.

Fletcher, R.S., Reddy, K.N., 2016. Random forest and leaf multispectral reflectance data to differentiate three soybean varieties from two pigweeds. Comput. Electron. Agric. 128, 199–206. https://doi.org/10.1016/j.compag.2016.09.004.

Fowler, J.E., 2014. Compressive pushbroom and whiskbroom sensing for hyperspectral remote-sensing imaging. IEEE International Conference on Image Processing (ICIP) 2014, 684–688. https://doi.org/10.1109/ICIP.2014.7025137.

Gao, J.W., Chen, Z.C., Gao, L.R., Zhang, B., Ieee, (2016).GPU implementation of ant colony optimization-based band selections for hyperspectral data classification. 8th Workshop on Hyperspectral Image and Signal Processing - Evolution in Remote Sensing (WHISPERS). DOI: 10.1109/WHISPERS.2016.8071720.

Gao, Z., Shao, Y., Xuan, G., Wang, Y., Liu, Y., Han, X., 2020. Real-time hyperspectral imaging for the in-field estimation of strawberry ripeness with deep learning. Artif. Intell. Agric. 4, 31–38. https://doi.org/10.1016/j.aiia.2020.04.003.

García-Santillán, I.D., Montalvo, M., Guerrero, J.M., Pajares, G., 2017. Automatic detection of curved and straight crop rows from images in maize fields. Biosys. Eng. 156, 61–79. https://doi.org/10.1016/j.biosystemseng.2017.01.013.

Goel, P.K., Prasher, S.O., Landry, J.A., Patel, R.M., Bonnell, R.B., Viau, A.A., Miller, J.R., 2003a. Potential of airborne hyperspectral remote sensing to detect nitrogen deficiency and weed infestation in corn. Comput. Electron. Agric. 38 (2), 99–124. https://doi.org/10.1016/S0168-1699(02)00138-2.

Goel, P.K., Prasher, S.O., Patel, R.M., Landry, J.A., Bonnell, R.B., Viau, A.A., 2003b. Classification of hyperspectral data by decision trees and artificial neural networks to identify weed stress and nitrogen status of corn. Comput. Electron. Agric. 39 (2), 67–93. https://doi.org/10.1016/S0168-1699(03)00020-6.

Gómez-Casero, M.T., Castillejo-González, I.L., García-Ferrer, A., Peña-Barragán, J.M., Jurado-Expósito, M., García-Torres, L., López-Granados, F., 2010. Spectral discrimination of wild oat and canary grass in wheat fields for less herbicide application. Agron. Sustain. Dev. 30 (3), 689–699. https://doi.org/10.1051/agro/2009052.

González, C., Sánchez, S., Paz, A., Resano, J., Mozos, D., Plaza, A., 2013. Use of FPGA or GPU-based architectures for remotely sensed hyperspectral image processing. Integration 46 (2), 89–103. https://doi.org/10.1016/j.vlsi.2012.04.002.

Gupta, O., Raskar, R., 2018. Distributed learning of deep neural network over multiple agents. J. Netw. Comput. Appl. 116, 1–8. https://doi.org/10.1016/j.jnca.2018.05.003.

Gyaneshwar, D., Nidamanuri, R.R., 2022. A real-time FPGA accelerated stream processing for hyperspectral image classification. GeoIn 37 (1), 52–69. https://doi.org/10.1080/10106049.2020.1713231.

Haddaway, N.R., Page, M.J., Pritchard, C.C., McGuinness, L.A., 2022. PRISMA2020: An r package and shiny app for producing PRISMA 2020-compliant flow diagrams, with interactivity for optimised digital transparency and open synthesis. Campbell Syst. Rev. 18 (2), e1230.

Haut, J.M., Paoletti, M.E., Plaza, J., Plaza, A., Li, J., 2019. Hyperspectral image classification using random occlusion data augmentation. IEEE Geosci. Remote Sens. Lett. 16 (11), 1751–1755. https://doi.org/10.1109/LGRS.2019.2909495.

He, H.-J., Sun, D.-W., 2015. Hyperspectral imaging technology for rapid detection of various microbial contaminants in agricultural and food products. Trends Food Sci. Technol. 46 (1), 99–109. https://doi.org/10.1016/j.tifs.2015.08.001.

Herrmann, I., Shapira, U., Kinast, S., Karnieli, A., Bonfil, D.J., 2013. Ground-level hyperspectral imagery for detecting weeds in wheat fields. Precis. Agric. 14 (6), 637–659. https://doi.org/10.1007/s11119-013-9321-x.

Horstrand, P., Guerra, R., DÍaz, M., Morales, A., Jiménez, A., López, S., López, J.F., 2019a. A spectral imaging system for precision agriculture: From its inception till a pre-commercial prototype. 2019 XXXIV Conference on Design of Circuits and Integrated Systems (DCIS). 1-6. DOI: 10.1109/DCIS201949030.2019.8959891.

Horstrand, P., Guerra, R., Rodriguez, A., Diaz, M., Lopez, S., Lopez, J.F., 2019b. A UAV platform based on a hyperspectral sensor for image capturing and on-board processing. IEEE Access 7, 66919–66938. https://doi.org/10.1109/access.2019.2913957.

Hou, L., Cheng, Y., Shazeer, N., Parmar, N., Li, Y., Korfiatis, P., Drucker, T.M., Blezek, D. J., Song, X., 2019. High resolution medical image analysis with spatial partitioning. arXiv preprint arXiv:1909.03108. DOI: 10.48550/arXiv.1909.03108.

Huang, L., Liu, Y., Huang, W., Dong, Y., Ma, H., Wu, K., Guo, A., 2022. Combining random forest and XGboost methods in detecting early and mid-term winter wheat

stripe rust using canopy level hyperspectral measurements. Agriculture 12 (1), 74. https://doi.org/10.3390/agriculture12010074.
Hutto, K.C., Shaw, D.R., Byrd, J.D., King, R.L., 2006. Differentiation of turfgrass and common weed species using hyperspectral radiometry. Weed Sci. 54 (2), 335–339. https://doi.org/10.1614/WS-05-116R.1.
Isaksson, T., Næs, T., 1988. The effect of multiplicative scatter correction (MSC) and linearity improvement in NIR spectroscopy. Appl. Spectrosc. 42 (7), 1273–1284. https://doi.org/10.1366/0003702884429869.
Jarolmasjed, S., Sankaran, S., Kalcsits, L., Khot, L.R., 2018. Proximal hyperspectral sensing of stomatal conductance to monitor the efficacy of exogenous abscisic acid applications in apple trees. Crop Protect. 109, 42–50. https://doi.org/10.1016/j.cropro.2018.02.022.
Jiang, J., Zhu, J., Wang, X., Cheng, T., Tian, Y., Zhu, Y., Cao, W., Yao, X., 2021. Estimating the leaf nitrogen content with a new feature extracted from the ultra-high spectral and spatial resolution images in wheat. Remote Sens. 13 (4), 739. https://doi.org/10.3390/rs13040739.
Jordan, M.I., Mitchell, T.M., 2015. Machine learning: Trends, perspectives, and prospects. Science 349 (6245), 255–260. https://doi.org/10.1126/science.aaa8415.
Junttila, S., Holtta, T., Saarinen, N., Kankare, V., Yrttimaa, T., Hyyppa, J., Vastaranta, M., 2022. Close-range hyperspectral spectroscopy reveals leaf water content dynamics. Remote Sens. Environ. 277 (13), 113071 https://doi.org/10.1016/j.rse.2022.113071.
Kaarna, A., Ohinata, G., Dutta, A., 2007. Compression of spectral images. I-Tech Education and Publishing. http://www.intechopen.com/books/vision_systems_segmentation_and_pattern_recognition/compression_of_spectral_images.
Khan, A., Vibhute, A.D., Mali, S., Patil, C.H., 2022. A systematic review on hyperspectral imaging technology with a machine and deep learning methodology for agricultural applications. Ecol. Inform. 69, 101678 https://doi.org/10.1016/j.ecoinf.2022.101678.
Kim, M., Chen, Y., Mehl, P., 2001. Hyperspectral reflectance and fluorescence imaging system for food quality and safety. Trans. ASAE 44 (3), 721. https://doi.org/10.13031/2013.6099.
Langer, M., He, Z., Rahayu, W., Xue, Y., 2020. Distributed training of deep learning models: A taxonomic perspective. IEEE Trans. Parallel Distrib. Syst. 31 (12), 2802–2818. https://doi.org/10.1109/TPDS.2020.3003307.
Li, Y., Al-Sarayreh, M., Irie, K., Hackell, D., Bourdot, G., Reis, M.M., Ghamkhar, K., 2021. Identification of weeds based on hyperspectral imaging and machine learning [Original Research]. Front. Plant Sci. 11 https://doi.org/10.3389/fpls.2020.611622.
Li, S., Wu, H., Wan, D., Zhu, J., 2011. An effective feature selection method for hyperspectral image classification based on genetic algorithm and support vector machine. Knowl.-Based Syst. 24 (1), 40–48. https://doi.org/10.1016/j.knosys.2010.07.003.
Lu, B., Dao, P.D., Liu, J., He, Y., Shang, J., 2020. Recent advances of hyperspectral imaging technology and applications in agriculture. Remote Sensing 12 (16), 2659. https://www.mdpi.com/2072-4292/12/16/2659.
Luo, L., Chang, Q., Gao, Y., Jiang, D., Li, F., 2022. Combining different transformations of ground hyperspectral data with unmanned aerial vehicle (UAV) images for anthocyanin estimation in tree peony leaves. Remote Sens. 14 (9), 2271. https://doi.org/10.3390/rs14092271.
Ma, S., Li, Y., Peng, Y., 2023. Spectroscopy and computer vision techniques for noninvasive analysis of legumes: A review. Comput. Electron. Agric. 206, 107695 https://doi.org/10.1016/j.compag.2023.107695.
Machidon, A.L., Machidon, O.M., Ciobanu, C.B., Ogrutan, P.L., 2020. Accelerating a geometrical approximated PCA algorithm using AVX2 and CUDA. Remote Sens., 12 (12), Article 1918. DOI: 10.3390/rs12121918.
Maes, W.H., Steppe, K., 2019. Perspectives for remote sensing with unmanned aerial vehicles in precision agriculture. Trends Plant Sci. 24 (2), 152–164. https://doi.org/10.1016/j.tplants.2018.11.007.
Martel, E., Lazcano, R., Lopez, J., Madronal, D., Salvador, R., Lopez, S., Juarez, E., Guerra, R., Sanz, C., Sarmiento, R., 2018. Implementation of the principal component analysis onto high-performance computer facilities for hyperspectral dimensionality reduction: Results and comparisons. Remote Sens. 10 (6), 864 https://doi.org/10.3390/rs10060864.
Matzrafi, M., Herrmann, I., Nansen, C., Kliper, T., Zait, Y., Ignat, T., Siso, D., Rubin, B., Karnieli, A., Eizenberg, H., 2017. Hyperspectral technologies for assessing seed germination and trifloxysulfuron-methyl response in amaranthus palmeri (palmer amaranth) [Original Research]. Front Plant Sci. 8 (474) https://doi.org/10.3389/fpls.2017.00474.
Merfield, C.N., 2016. Robotic weeding's false dawn? Ten requirements for fully autonomous mechanical weed management. Weed Res. 56 (5), 340–344. https://doi.org/10.1111/wre.12217.
Mertens, S., Verbraeken, L., Sprenger, H., Demuynck, K., Maleux, K., Cannoot, B., De Block, J., Maere, S., Nelissen, H., Bonaventure, G., Crafts-Brandner, S.J., Vogel, J.T., Bruce, W., Inze, D., Wuyts, N., 2021. Proximal hyperspectral imaging detects diurnal and drought-induced changes in maize physiology. Front. Plant Sci. 12 (18), 640914 https://doi.org/10.3389/fpls.2021.640914.
Miguel, A.C., Ladner, R.E., Riskin, E.A., Hauck, S., Barney, D.K., Askew, A.R., Chang, A., 2006. Predictive coding of hyperspectral images. Hyperspectral Data Compression 197–231. https://doi.org/10.1007/0-387-28600-4_8.
Mishra, P., Asaari, M.S.M., Herrero-Langreo, A., Lohumi, S., Diezma, B., Scheunders, P., 2017b. Close range hyperspectral imaging of plants: A review. Biosys. Eng. 164, 49–67. https://doi.org/10.1016/j.biosystemseng.2017.09.009.
Mishra, A., Rajput, N.S., Singh, K.P., Singh, D., Ieee, 2017a. An object linked intelligent classification method for hyperspectral images. IEEE International Geoscience and Remote Sensing Symposium (IGARSS). 3345-3348. DOI: 10.1109/IGARSS.2017.8127714.
Mishra, P., Lohumi, S., Ahmad Khan, H., Nordon, A., 2020. Close-range hyperspectral imaging of whole plants for digital phenotyping: Recent applications and illumination correction approaches. Comput. Electron. Agric. 178 https://doi.org/10.1016/j.compag.2020.105780.
Mishra, P., Passos, D., Marini, F., Xu, J., Amigo, J.M., Gowen, A.A., Jansen, J.J., Biancolillo, A., Roger, J.M., Rutledge, D.N., Nordon, A., 2022a. Deep learning for near-infrared spectral data modelling: Hypes and benefits. TrAC, Trends Anal. Chem. 157, 116804 https://doi.org/10.1016/j.trac.2022.116804.
Mishra, P., Sytsma, M., Chauhan, A., Polder, G., Pekkeriet, E., 2022b. All-in-one: A spectral imaging laboratory system for standardised automated image acquisition and real-time spectral model deployment. Anal. Chim. Acta 1190, 339235. https://doi.org/10.1016/j.aca.2021.339235.
Mo, C., Kim, G., Lee, K., Kim, M.S., Cho, B.-K., Lim, J., Kang, S., 2014. Non-destructive quality evaluation of pepper (capsicum annuum l.) seeds using LED-induced hyperspectral reflectance imaging. Sensors 14 (4), 7489–7504. https://doi.org/10.3390/s140407489.
Mobaraki, N., Amigo, J.M., 2018. HYPER-Tools. A graphical user-friendly interface for hyperspectral image analysis. Chemometrics Intellig. Lab. Syst. 172, 174–187. https://doi.org/10.1016/j.chemolab.2017.11.003.
Mohan, A., Venkatesan, M., 2020. Hybrid dimensionality reduction technique for hyperspectral images using random projection and manifold learning. 24th Pacific-Asia Conference on Knowledge Discovery and Data Mining (PAKDD). 116-127. DOI: 10.1007/978-3-030-60470-7_12.
Nagasubramanian, K., Jones, S., Singh, A.K., Sarkar, S., Singh, A., Ganapathysubramanian, B., 2019. Plant disease identification using explainable 3D deep learning on hyperspectral images. Plant Methods 15 (1), 98. https://doi.org/10.1186/s13007-019-0479-8.
Nalepa, J., Myller, M., Kawulok, M., (2019). Hyperspectral data augmentation. arXiv preprint arXiv:1903.05580. DOI: 10.48550/arXiv.1903.05580.
Nascimento, J.M.P., Vestias, M., Martin, G., Ieee, 2015. FPGA-based architecture for hyperspectral unmixing. IEEE International Geoscience and Remote Sensing Symposium (IGARSS). 1761-1764. DOI: 10.1109/IGARSS.2015.7326130.
Nascimento, J.M.P., Vestias, M., 2016. System-on-chip field-programmable gate array design for onboard real-time hyperspectral unmixing. J. Appl. Remote Sens. 10, 015004 https://doi.org/10.1117/1.Jrs.10.015004.
Nascimento, J.M.P., Véstias, M.P., Martín, G., 2020. Hyperspectral compressive sensing with a system-on-chip FPGA. IEEE J. Sel. Top. Appl. Earth Obs. Remote Sens. 13, 3701–3710. https://doi.org/10.1109/JSTARS.2020.2996679.
Nie, C., Shi, L., Li, Z., Xu, X., Yin, D., Li, S., Jin, X., 2023. A comparison of methods to estimate leaf area index using either crop-specific or generic proximal hyperspectral datasets. Eur. J. Agron. 142, 126664 https://doi.org/10.1016/j.eja.2022.126664.
Okamoto, H., Murata, T., Kataoka, T., Hata, S.-I., 2007. Plant classification for weed detection using hyperspectral imaging with wavelet analysis. Weed Biol. Manage. 7 (1), 31–37. https://doi.org/10.1111/j.1445-6664.2006.00234.x.
Omidi, R., Pourreza, A., Moghimi, A., Zuniga-Ramirez, G., Jafarbiglu, H., Maung, Z., Westphal, A., 2022. A semi-supervised approach to cluster symptomatic and asymptomatic leaves in root lesion nematode infected walnut trees. Comput. Electron. Agric. 194 (8), 106761 https://doi.org/10.1016/j.compag.2022.106761.
Osborne, B.G., 1993. Practical NIR spectroscopy with applications in food and beverage analysis. Longman Sci. Tech.
Page, M.J., McKenzie, J.E., Bossuyt, P.M., Boutron, I., Hoffmann, T.C., Mulrow, C.D., Shamseer, L., Tetzlaff, J.M., Akl, E.A., Brennan, S.E., Chou, R., Glanville, J., Grimshaw, J.M., Hróbjartsson, A., Lalu, M.M., Li, T., Loder, E.W., Mayo-Wilson, E., McDonald, S., McGuinness, L.A., Stewart, L.A., Thomas, J., Tricco, A.C., Welch, V.A., Whiting, P., Moher, D., 2021. The PRISMA 2020 statement: An updated guideline for reporting systematic reviews. Syst. Rev. 10 (1), 89. https://doi.org/10.1186/s13643-021-01626-4.
Pantazi, X.-E., Moshou, D., Bravo, C., 2016. Active learning system for weed species recognition based on hyperspectral sensing. Biosys. Eng. 146, 193–202. https://doi.org/10.1016/j.biosystemseng.2016.01.014.
Park, K., Ki Hong, Y., Hwan Kim, G., Lee, J., 2018. Classification of apple leaf conditions in hyper-spectral images for diagnosis of marssonina blotch using mRMR and deep neural network. Comput. Electron. Agric. 148, 179–187. https://doi.org/10.1016/j.compag.2018.02.025.
Passos, D., Mishra, P., 2022. A tutorial on automatic hyperparameter tuning of deep spectral modelling for regression and classification tasks. Chemometrics Intellig. Lab. Syst. 223, 104520 https://doi.org/10.1016/j.chemolab.2022.104520.
Pavia, D.L., Lampman, G.M., Kriz, G.S., Vyvyan, J.A., 2014. Introduction to spectroscopy. Cengage Learning. https://doi.org/10.1021/ed056pa323.2.
Peerbhay, K., Mutanga, O., Lottering, R., Bangamwabo, V., Ismail, R., 2016. Detecting bugweed (solanum mauritianum) abundance in plantation forestry using multisource remote sensing. ISPRS J. Photogramm. Remote Sens. 121, 167–176. https://doi.org/10.1016/j.isprsjprs.2016.09.014.
Peña-Barragán, J.M., López-Granados, F., Jurado-Expósito, M., García-Torres, L., 2006. Spectral discrimination of ridolfia segetum and sunflower as affected by phenological stage. Weed Res. 46 (1), 10–21. https://doi.org/10.1111/j.1365-3180.2006.00488.x.
Penalver, M., Del Frate, F., Paoletti, M.E., Haut, J.M., Plaza, J., Plaza, A., Ieee, 2017. Onboard payload-data dimensionality reduction. IEEE International Geoscience & Remote Sensing Symposium 783–786. https://doi.org/10.1109/IGARSS.2017.8127069.
Picon, A., Bereciartua, A., Echazarra, J., Ghita, O., Whelan, P., Iriondo, P., 2012. Real-time hyperspectral processing for automatic nonferrous material sorting. JEI 21 (1), 013018. https://doi.org/10.1117/1.JEI.21.1.013018.

Polder, G., Blok, P.M., de Villiers, H.A.C., van der Wolf, J.M., Kamp, J., 2019. Potato virus y detection in seed potatoes using deep learning on hyperspectral images [Original Research]. Front. Plant Sci. 10 https://doi.org/10.3389/fpls.2019.00209.
Qi, C., Sandroni, M., Westergaard, J.C., Sundmark, E.H.R., Bagge, M., Alexandersson, E., Gao, J., 2023. In-field classification of the asymptomatic biotrophic phase of potato late blight based on deep learning and proximal hyperspectral imaging. Comput. Electron. Agric. 205, 107585 https://doi.org/10.1016/j.compag.2022.107585.
Qin, J., 2010. Chapter 5 - hyperspectral imaging instruments. In: Sun, D.-.-W. (Ed.), Hyperspectral Imaging for Food Quality Analysis and Control. Academic Press, San Diego, pp. 129–172. https://doi.org/10.1016/B978-0-12-374753-2.10005-X.
Reddy, K.N., Huang, Y., Lee, M.A., Nandula, V.K., Fletcher, R.S., Thomson, S.J., Zhao, F., 2014. Glyphosate-resistant and glyphosate-susceptible palmer amaranth (amaranthus palmeri s. Wats.): Hyperspectral reflectance properties of plants and potential for classification. Pest Manage. Sci. 70 (12), 1910–1917. https://doi.org/10.1002/ps.3755.
Rinnan, Å., Nørgaard, L., van den Berg, F., Thygesen, J., Bro, R., Engelsen, S.B., 2009. Data Pre-Processing. https://doi.org/10.1016/b978-0-12-374136-3.00002-x.
Rochac, J.F.R., Zhang, N., Thompson, L., Oladunni, T., 2019. A data augmentation-assisted deep learning model for high dimensional and highly imbalanced hyperspectral imaging data. 2019 9th International Conference on Information Science and Technology (ICIST). 362-367. DOI: 10.1109/ICIST.2019.8836913.
Rosario, J., Nascimento, J.M.P., Vestias, M., (2014).FPGA-based architecture for hyperspectral endmember extraction. Conference on High-Performance Computing in Remote Sensing IV. DOI: 10.1117/12.2067039.
Rubio-Delgado, J., Pérez, C.J., Vega-Rodríguez, M.A., 2021. Predicting leaf nitrogen content in olive trees using hyperspectral data for precision agriculture. Precis. Agric. 22 (1), 1–21. https://doi.org/10.1007/s11119-020-09727-1.
Sanaeifar, A., Yang, C., de la Guardia, M., Zhang, W., Li, X., He, Y., 2023. Proximal hyperspectral sensing of abiotic stresses in plants. Sci. Total Environ. 861, 160652 https://doi.org/10.1016/j.scitotenv.2022.160652.
Sanchez, S., Plaza, A., 2011. Real-time implementation of a full hyperspectral unmixing chain on graphics processing units. Conference on Satellite Data Compression, Communications, and Processing VII. https://doi.org/10.1117/12.892284.
Savitzky, A., Golay, M.J., 1964. Smoothing and differentiation of data by simplified least squares procedures. Anal. Chem. 36 (8), 1627–1639. https://doi.org/10.1021/ac60214a047.
Sergeev, A., Del Balso, M., (2018). Horovod: Fast and easy distributed deep learning in tensorflow. arXiv preprint arXiv:1802.05799. DOI: 10.48550/arXiv.1802.05799.
Sevilla, L., Martin, G., Nascimento, J., Bioucas-Dias, J., Ieee, (2016).Hyperspectral image reconstruction from random projections on GPU. 36th IEEE International Geoscience and Remote Sensing Symposium (IGARSS). 280-283. DOI: 10.1109/igarss.2016.7729064.
Shazeer, N., Cheng, Y., Parmar, N., Tran, D., Vaswani, A., Koanantakool, P., Hawkins, P., Lee, H., Hong, M., Young, C., 2018. Mesh-tensorflow: Deep learning for supercomputers. Adv. Neural Inf. Process Syst. 31.
Shibi, C.S., Gayathri, R., 2021. Onboard target detection in hyperspectral image based on deep learning with FPGA implementation. Microprocess. Microsyst. 85 https://doi.org/10.1016/j.micpro.2021.104313.
Shirzadifar, A., Bajwa, S., Mireei, S.A., Howatt, K., Nowatzki, J., 2018. Weed species discrimination based on SIMCA analysis of plant canopy spectral data. Biosys. Eng. 171, 143–154. https://doi.org/10.1016/j.biosystemseng.2018.04.019.
Shuaibu, M., Lee, W.S., Schueller, J., Gader, P., Hong, Y.K., Kim, S., 2018. Unsupervised hyperspectral band selection for apple marssonina blotch detection. Comput. Electron. Agric. 148, 45–53. https://doi.org/10.1016/j.compag.2017.09.038.
Siedliska, A., Baranowski, P., Mazurek, W., 2014. Classification models of bruise and cultivar detection on the basis of hyperspectral imaging data. Comput. Electron. Agric. 106, 66–74. https://doi.org/10.1016/j.compag.2014.05.012.
Singh, H., Roy, A., Setia, R.K., Pateriya, B., 2022. Estimation of nitrogen content in wheat from proximal hyperspectral data using machine learning and explainable artificial intelligence (XAI) approach. Model. Earth Syst. Environ. 8 (2), 2505–2511. https://doi.org/10.1007/s40808-021-01243-z.
Sousa, J.J., Toscano, P., Matese, A., Di Gennaro, S.F., Berton, A., Gatti, M., Poni, S., Pádua, L., Hruška, J., Morais, R., Peres, E., 2022. UAV-based hyperspectral monitoring using push-broom and snapshot sensors: A multisite assessment for precision viticulture applications. Sensors 22 (17), 6574. https://www.mdpi.com/1424-8220/22/17/6574.
Su, J., Yi, D., Coombes, M., Liu, C., Zhai, X., McDonald-Maier, K., Chen, W.-H., 2022. Spectral analysis and mapping of blackgrass weed by leveraging machine learning and UAV multispectral imagery. Comput. Electron. Agric. 192, 106621 https://doi.org/10.1016/j.compag.2021.106621.
Suzuki, Y., Okamoto, H., Kataoka, T., 2008. Image segmentation between crop and weed using hyperspectral imaging for weed detection in soybean field. Environ. Control. Biol. 46 (3), 163–173. https://doi.org/10.2525/ecb.46.163.
Symonds, P., Paap, A., Alameh, K., Rowe, J., Miller, C., 2015. A real-time plant discrimination system utilising discrete reflectance spectroscopy. Comput. Electron. Agric. 117, 57–69. https://doi.org/10.1016/j.compag.2015.07.011.
Tan, H., Hu, Y., Ma, B., Yu, G., Li, Y., 2024. An improved DCGAN model: Data augmentation of hyperspectral image for identification pesticide residues of hami melon. Food Control 157, 110168. https://doi.org/10.1016/j.foodcont.2023.110168.
Tao, F., Yao, H., Hruska, Z., Burger, L.W., Rajasekaran, K., Bhatnagar, D., 2018. Recent development of optical methods in rapid and non-destructive detection of aflatoxin and fungal contamination in agricultural products. TrAC. Trends Anal. Chem. 100, 65–81. https://doi.org/10.1016/j.trac.2017.12.017.
Tarabalka, Y., Haavardsholm, T.V., Kåsen, I., Skauli, T., 2009. Real-time anomaly detection in hyperspectral images using multivariate normal mixture models and GPU processing. J. Real-Time Image Pr. 4 (3), 287–300. https://doi.org/10.1007/s11554-008-0105-x.
Tatzer, P., Wolf, M., Panner, T., 2005. Industrial application for inline material sorting using hyperspectral imaging in the NIR range. RTI 11 (2), 99–107. https://doi.org/10.1016/j.rti.2005.04.003.
Thomas, S., Kuska, M.T., Bohnenkamp, D., Brugger, A., Alisaac, E., Wahabzada, M., Behmann, J., Mahlein, A.-K., 2018. Benefits of hyperspectral imaging for plant disease detection and plant protection: A technical perspective. J. Plant Dis. Prot. 125 (1), 5–20. https://doi.org/10.1007/s41348-017-0124-6.
Thorp, K.R., Gore, M.A., Andrade-Sanchez, P., Carmo-Silva, A.E., Welch, S.M., White, J.W., French, A.N., 2015. Proximal hyperspectral sensing and data analysis approaches for field-based plant phenomics. Comput. Electron. Agric. 118, 225–236. https://doi.org/10.1016/j.compag.2015.09.005.
Torti, E., Acquistapace, M., Danese, G., Leporati, F., Plaza, A., 2014. Real-time identification of hyperspectral subspaces. IEEE J. Sel. Top. Appl. Earth Obs. Remote Sens. 7 (6), 2680–2687. https://doi.org/10.1109/jstars.2014.2304832.
Van De Vijver, R., Mertens, K., Heungens, K., Somers, B., Nuyttens, D., Borra-Serrano, I., Lootens, P., Roldán-Ruiz, I., Vangeyte, J., Saeys, W., 2020. In-field detection of alternaria solani in potato crops using hyperspectral imaging. Comput. Electron. Agric. 168, 105106 https://doi.org/10.1016/j.compag.2019.105106.
Vigneau, N., Ecarnot, M., Rabatel, G., Roumet, P., 2011. Potential of field hyperspectral imaging as a non destructive method to assess leaf nitrogen content in wheat. Field Crops Res. 122 (1), 25–31. https://doi.org/10.1016/j.fcr.2011.02.003.
Virlet, N., Sabermanesh, K., Sadeghi-Tehran, P., Hawkesford, M.J., 2017. Field scanalyzer: An automated robotic field phenotyping platform for detailed crop monitoring [Review]. Funct. Plant Biol. 44 (1), 143–153. https://doi.org/10.1071/FP16163.
Wang, T., Gao, M., Cao, C., You, J., Zhang, X., Shen, L., 2022. Winter wheat chlorophyll content retrieval based on machine learning using in situ hyperspectral data. Comput. Electron. Agric. 193, 106728 https://doi.org/10.1016/j.compag.2022.106728.
Wang, C., Liu, B., Liu, L., Zhu, Y., Hou, J., Liu, P., Li, X., 2021. A review of deep learning used in the hyperspectral image analysis for agriculture. Artif. Intell. Rev. 54 (7), 5205–5253. https://doi.org/10.1007/s10462-021-10018-y.
Wei, D., Huang, Y., Chunjiang, Z., Xiu, W., 2015. Identification of seedling cabbages and weeds using hyperspectral imaging. Int. J. Agric. Biol. Eng. 8 (5), 65–72. https://doi.org/10.3965/j.ijabe.20150805.1492.
Wei, X., Johnson, M.A., Langston, D.B., Mehl, H.L., Li, S., 2021. Identifying optimal wavelengths as disease signatures using hyperspectral sensor and machine learning. Remote Sens. 13 (14), 2833 https://doi.org/10.3390/rs13142833.
Wieme, J., Mollazade, K., Malounas, I., Zude-Sasse, M., Zhao, M., Gowen, A., Argyropoulos, D., Fountas, S., Van Beek, J., 2022. Application of hyperspectral imaging systems and artificial intelligence for quality assessment of fruit, vegetables and mushrooms: A review. Biosys. Eng. 222, 156–176. https://doi.org/10.1016/j.biosystemseng.2022.07.013.
Williams, D., Britten, A., McCallum, S., Jones, H., Aitkenhead, M., Karley, A., Loades, K., Prashar, A., Graham, J., 2017. A method for automatic segmentation and splitting of hyperspectral images of raspberry plants collected in field conditions. Plant Methods 13 (1), 74. https://doi.org/10.1186/s13007-017-0226-y.
Wong, G., 2009. Snapshot hyperspectral imaging and practical applications. J. Phys. Conf. Ser. 178 (1), 012048 https://doi.org/10.1088/1742-6596/178/1/012048.
Xiao, Z., Wang, J., 2020. Rapid nondestructive defect detection of scindapsus aureus leaves based on PCA spectral feature optimization. IOP Conf. Ser.: Earth Environ. Sci., 032018 https://doi.org/10.1088/1755-1315/440/3/032018.
Xu, R.L., Gao, C., Jiang, J.F., 2018. Study of multilevel parallel algorithm of KPCA for hyperspectral images. 36th National Conference of Theoretical Computer Science (NCTCS). 99-115. DOI: 10.1007/978-981-13-2712-4_8.
Xu, J.-L., Riccioli, C., Herrero-Langreo, A., Gowen, A.A., 2020. Deep learning classifiers for near infrared spectral imaging: A tutorial. J. Spectr. Imaging 9. https://doi.org/10.1255/jsi.2020.a19.
Xue, B., Tian, L., Wang, Z., Wang, X., Yao, X., Zhu, Y., Cao, W., Cheng, T., 2023. Quantification of rice spikelet rot disease severity at organ scale with proximal imaging spectroscopy. Precis. Agric. https://doi.org/10.1007/s11119-022-09987-z.
Xue, T.R., Wang, Y.M., Chen, Y.W., Jia, J.X., Wen, M.X., Guo, R., Wu, T.X., Deng, X., 2021. Mixed noise estimation model for optimized kernel minimum noise fraction transformation in hyperspectral image dimensionality reduction. Remote Sens. 13 (13), 2607 https://doi.org/10.3390/rs13132607.
Yang, H., Du, Q., Ieee, 2011. Fast band selection for hyperspectral imagery. 17th IEEE International Conference on Parallel and Distributed Systems (ICPADS). 1048-1051. DOI: 10.1109/icpads.2011.157.
Yong, L.Z., Khairunniza-Bejo, S., Jahari, M., Muharam, F.M., 2023. Automatic disease detection of basal stem rot using deep learning and hyperspectral imaging. Agriculture 13 (1), 69. https://doi.org/10.3390/agriculture13010069.
Yu, K.Q., Fang, S.Y., Zhao, Y.R., 2021. Heavy metal hg stress detection in tobacco plant using hyperspectral sensing and data-driven machine learning methods. Spectrochim. Acta. Part A at. Spectrosc. 245 (12), 118917 https://doi.org/10.1016/j.saa.2020.118917.
Zahavi, A., Palshin, A., Liyanage, D.C., Tamre, M., 2019. Influence of illumination sources on hyperspectral imaging. 2019 20th International Conference on Research and Education in Mechatronics (REM). 1-5. DOI: 10.1109/REM.2019.8744086.
Zhang, Y., Gao, J., Cen, H., Lu, Y., Yu, X., He, Y., Pieters, J.G., 2019b. Automated spectral feature extraction from hyperspectral images to differentiate weedy rice and barnyard grass from a rice crop. Comput. Electron. Agric. 159, 42–49. https://doi.org/10.1016/j.compag.2019.02.018.
Zhang, X., Han, L., Dong, Y., Shi, Y., Huang, W., Han, L., González-Moreno, P., Ma, H., Ye, H., Sobeih, T., 2019a. A deep learning-based approach for automated yellow rust

disease detection from high-resolution hyperspectral UAV images. Remote Sens. 11 (13), 1554. https://doi.org/10.3390/rs11131554.

Zhang, L., Nie, Q., Ji, H., Wang, Y., Wei, Y., An, D., 2022. Hyperspectral imaging combined with generative adversarial network (GAN)-based data augmentation to identify haploid maize kernels. J. Food Compos. Anal. 106, 104346 https://doi.org/10.1016/j.jfca.2021.104346.

Zhang, Y., Slaughter, D.C., 2011. Hyperspectral species mapping for automatic weed control in tomato under thermal environmental stress. Comput. Electron. Agric. 77 (1), 95–104. https://doi.org/10.1016/j.compag.2011.04.001.

Zhang, Y., Slaughter, D.C., Staab, E.S., 2012a. Robust hyperspectral vision-based classification for multi-season weed mapping. ISPRS J. Photogramm. Remote Sens. 69, 65–73. https://doi.org/10.1016/j.isprsjprs.2012.02.006.

Zhang, Y., Staab, E.S., Slaughter, D.C., Giles, D.K., Downey, D., 2012b. Automated weed control in organic row crops using hyperspectral species identification and thermal micro-dosing. Crop Protect. 41, 96–105. https://doi.org/10.1016/j.cropro.2012.05.007.

Zhao, Q., Zhang, Z., Huang, Y., Fang, J., 2022. TPE-RBF-SVM model for soybean categories recognition in selected hyperspectral bands based on extreme gradient boosting feature importance values. Agriculture 12 (9), 1452. https://doi.org/10.3390/agriculture12091452.

Zhou, H.F., Gao, C., Liu, X.Y., 2017. Design and optimization of nonlinear dimensionality reduction algorithm for hyperspectral images on heterogeneous system. EEE International Conference on Internet of Things (iThings) and IEEE Green Computing and Communications (GreenCom) and IEEE Cyber, Physical and Social Computing (CPSCom) and IEEE Smart Data (SmartData). 1076-1081. DOI: 10.1109/iThings-GreenCom-CPSCom-SmartData.2017.164.

Zhu, W., Sun, Z., Yang, T., Li, J., Peng, J., Zhu, K., Li, S., Gong, H., Lyu, Y., Li, B., 2020. Estimating leaf chlorophyll content of crops via optimal unmanned aerial vehicle hyperspectral data at multi-scales. Comput. Electron. Agric. 178, 105786 https://doi.org/10.1016/j.compag.2020.105786.